

# Pre-exposure of abundant species to disturbance improves resilience in microbial metacommunities

Received: 9 January 2024

Accepted: 3 December 2024

Published online: 17 January 2025

 Check for updates

Johannes Cairns<sup>1,2,3,4</sup>, Shane Hogle<sup>1</sup>, Elizaveta Alitupa<sup>1</sup>, Ville Mustonen<sup>3,5</sup> & Teppo Hiltunen<sup>1</sup>✉

Understanding factors influencing community resilience to disturbance is critical for mitigating harm at various scales, including harm from medication to gut microbiota and harm from human activity to global biodiversity, yet there is a lack of data from large-scale controlled experiments. Factors expected to boost resilience include prior exposure to the same disturbance and dispersal from undisturbed patches. Here we set up an *in vitro* system to test the effect of disturbance pre-exposure and dispersal represented by community mixing. We performed a serial passage experiment on a 23-species bacterial model community, varying pre-exposure history and dispersal rate between three metacommunity patches subjected to different levels of disturbance by the antibiotic streptomycin. As expected, pre-exposure caused evolution of resistance, which prevented decrease in species abundance. The more abundant the pre-exposed species had been in the undisturbed community, the less the entire community changed. Pre-exposure of the most dominant species also decreased abundance change in off-target species. In the absence of pre-exposure, increasing dispersal rates caused increasing spread of the disturbance across the metacommunity. However, pre-exposure kept the metacommunity close to the undisturbed state regardless of dispersal rate. Our findings demonstrate that pre-exposure is an important modifier of ecological resilience in a metacommunity setting.

Ecological disturbances are events causing ecosystem change<sup>1</sup>. They vary in magnitude, frequency and extent, with durations ranging from discrete, short-term pulse disturbances to long-term or continuous press disturbances<sup>2,3</sup>. Currently, ecosystems on Earth are experiencing unprecedented disturbances owing to human activity. These include disturbances associated with global climate change, such as atmospheric increases in carbon dioxide, as well as those caused by using pesticides, herbicides and pharmaceuticals in agriculture and medicine.

To mitigate unwanted effects of ecological disturbances, it is critical to develop a mechanistic understanding of disturbance response<sup>4</sup>. In particular, this means understanding the conditions where disturbances compromise the structure or function, that is, the resilience of ecosystems. There exist two frameworks on resilience. The engineering resilience framework is focused on the return of a system to its pre-disturbance state, and can be partitioned into withstanding change during a disturbance (that is, ecological resistance) and

<sup>1</sup>Department of Biology, University of Turku, Turku, Finland. <sup>2</sup>Turku Collegium for Science, Medicine and Technology, University of Turku, Turku, Finland.

<sup>3</sup>Department of Computer Science, Organismal and Evolutionary Biology Research Programme, University of Helsinki, Helsinki, Finland. <sup>4</sup>Helsinki Institute of Sustainability Science (HELSUS), University of Helsinki, Helsinki, Finland. <sup>5</sup>Institute of Biotechnology, University of Helsinki, Helsinki, Finland.

✉e-mail: [teppo.hiltunen@utu.fi](mailto:teppo.hiltunen@utu.fi)

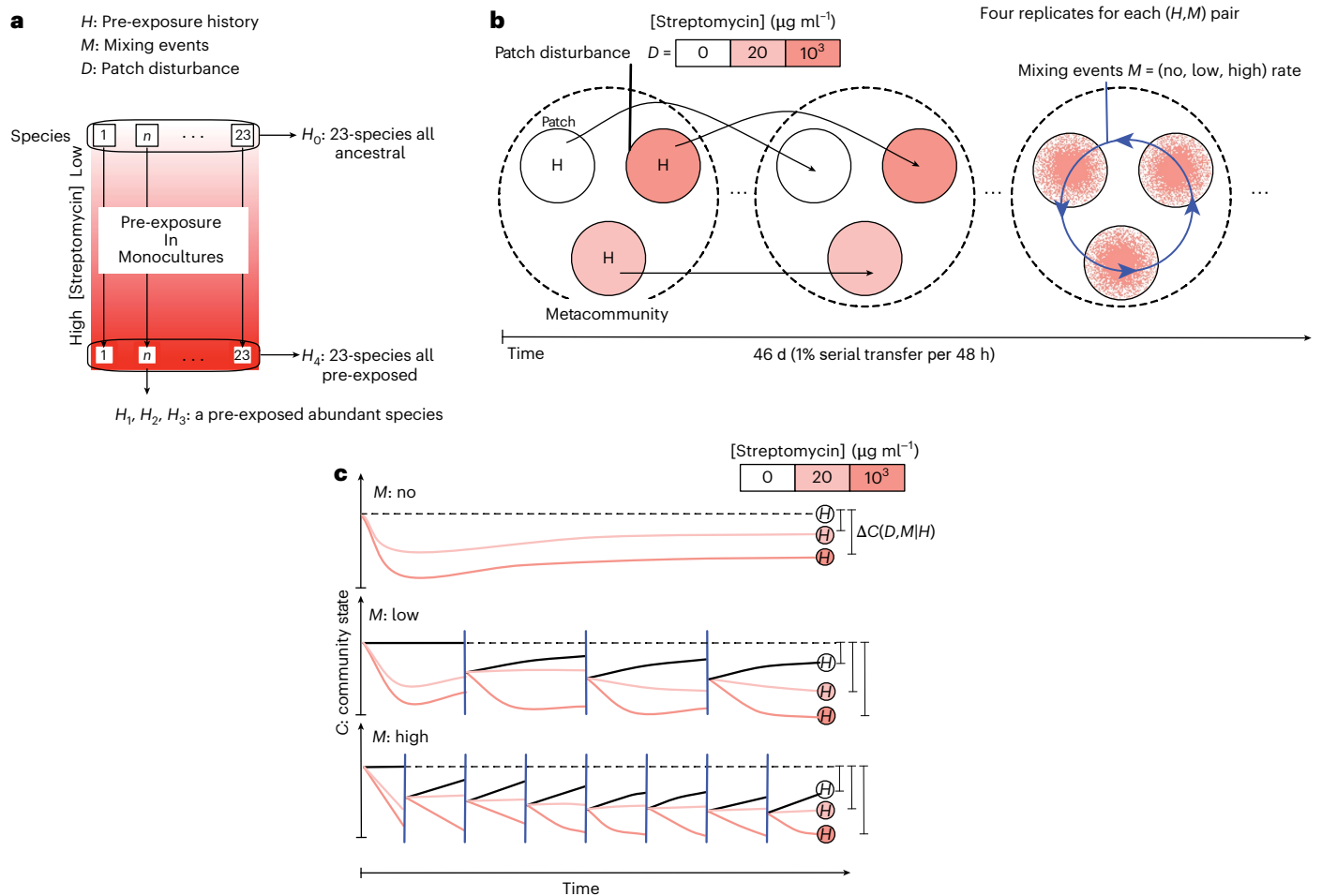


**Fig. 1 | Design of experiment to test effect of pre-exposure and community mixing rate on disturbance response in multispecies community.** **a**, The experimental system consisted of a 23-species bacterial model community where evolutionary history  $H$  was modified by pre-exposing each species in a monoculture to the disturbance, the antibiotic streptomycin and constructing communities with no pre-exposed species, one among three abundant species being pre-exposed or all 23 species being pre-exposed. **b**, These communities were each subjected to a regime of three rates of community mixing  $M$  (no, low or high) between three patches experiencing different levels of disturbance (patch harshness  $D$ : no, low or high antibiotic level), thereby constituting metacommunities. Each unique treatment combination was replicated four times, making up a total of 180 communities (five pre-exposure treatments,

three rates of community mixing, three disturbance patches and four replicates). Communities were serially passed (1% volume) to fresh medium every 48 h for 22 transfers (46 days). Low and high rates of community mixing (modelling connectivity and migration) were implemented by globally mixing communities from all three patches before serial transfer every three or six transfers, respectively. **c**, To test the study questions, high-throughput sequencing was used to quantify the community state  $C$  at the experimental end point, and clones were isolated to test for resistance phenotypes in the different treatments. These data were used to estimate divergence of communities  $\Delta C$  from the no-disturbance, no-mixing baseline (dashed horizontal line as measured at the experimental end point) within each pre-exposure history as a proxy for ecological resilience.

post-disturbance recovery<sup>5</sup>. The ecological resilience framework is focused on the degree and type of disturbance required to drive a system into a different state (that is, tipping point, causing a regime shift)<sup>6</sup>. In this study, we examine a system experiencing a constant press disturbance and therefore adopt the latter framework, seeking to identify conditions driving or preventing clear shifts in the system. It is critical to understand when a clear shift occurs in the state of an ecosystem as this can impair ecosystem functioning or even result in community collapse<sup>7–9</sup>.

Previous research has identified numerous factors influencing resilience in species communities, including disturbance intensity, frequency, timing and spatial extent, and the biological level affected<sup>9,10</sup>. Here we focus on two key factors: pre-exposure and dispersal. First, past disturbances (that is, pre-exposure) can prime communities to better cope with future disturbances through mechanisms including rapid trait evolution, epigenetics and maintenance of trait diversity (via genetic heterogeneity or phenotypic plasticity)<sup>9</sup>. In this study, we use rapidly evolving microorganisms, stressing the first

(and potentially last) of these mechanisms. While microorganisms are known to rapidly evolve resistance to various stressors in one- and two-species setups, only a few controlled studies have examined rapid microbial evolution or its ecological effects in larger communities<sup>11–15</sup>. We recently subjected a multispecies microorganism community to antibiotic pulse disturbance and found that the intrinsic competitive fitness and antibiotic susceptibility traits of the species primarily drove ecological changes despite the emergence of antibiotic resistance mutations<sup>16</sup>. However, in line with ecological literature, such evolutionary trait changes could affect the community response to future disturbances. To test this in the study at hand, we individually pre-exposed each species in a 23-species model bacterial community to gradually increasing and ultimately high levels of antibiotic disturbance, using the aminoglycoside antibiotic streptomycin. This was followed by phenotyping and whole-genome sequencing thus obtained populations to identify associated trait evolution. We then constructed communities with different pre-exposure histories for use in a serial passage experiment to test for disturbance response (Fig. 1a).

Dispersal is another critical factor affecting resilience. Communities are typically nested within patches in a metacommunity with varying magnitudes of dispersal (connectivity)<sup>17</sup>. Dispersal drives diversity, increasing local patch (alpha) diversity and decreasing meta-community (beta) diversity<sup>14,18</sup>. Dispersal varies in rate and scale, from small subpopulations to entire communities (community coalescence) common to microorganisms, with higher dispersal levels expected to strengthen dispersal effects<sup>19,20</sup>. However, not many studies have investigated the effect of dispersal rate on the disturbance response of communities. Findings from a recent study suggest that dispersal between communities experiencing low-level disturbance can improve community resilience (for example, restoring lost species), while dispersal between communities experiencing high-level disturbance can decrease community resilience (for example, driving extinction of weaker competitors)<sup>21</sup>. Dispersal from an undisturbed to a disturbed patch can boost resilience in a manner akin to source-sink dynamics<sup>16,22</sup>. By contrast, dispersal from a disturbed to an undisturbed patch can spread the eco-evolutionary effects of the disturbance to undisturbed communities<sup>23,24</sup>.

While the effects of pre-exposure to disturbance and dispersal on the community response to disturbance have received some attention, there is virtually no experimental evidence on the combined influence of these two factors. In the absence of pre-exposure, dispersal from disturbed patches should spread effects of the disturbance across the metacommunity. A higher dispersal rate should strengthen this effect. However, by boosting community resilience, pre-exposure to disturbance should also prevent change of the metacommunity. Higher dispersal rates should have little bearing on the outcome, potentially decreasing metacommunity diversity.

To test the effect of pre-exposure and dispersal rate on ecological resilience, we performed a full-factorial serial passage experiment for the 23-species model bacterial community with five pre-exposure histories: communities containing (1) only naive (ancestral) species, (2–4) a streptomycin pre-exposed population of one of three abundant species or (5) disturbance pre-exposed populations of all species (Fig. 1a). We divided each of the communities into three patches, subjected to no disturbance, low disturbance level or high disturbance level (different concentrations of streptomycin). To model the effect of connectivity level, we subjected the sets of patches to three rates of community mixing (global connectivity, with entire communities from all three patches mixed): no, low (every sixth transfer) and high (every third transfer). The three patches subject to mixing constitute metacommunities. We collected ecological and phenotypic data for species frequencies and antibiotic resistance for communities at the end point of the serial transfer experiment, allowing us to test the conditions driving or preventing community change (Fig. 1b).

## Results

### Pre-exposure to disturbance caused trait evolution

We used a synthetic community of 23 Gram-negative bacterial species isolated from soil, aquatic, plant, animal and human sources, as described earlier<sup>25</sup>. Most community members display quasi-stable co-existence over dozens of serial transfers<sup>16,25,26</sup>. As the species have been isolated from different environments, the presence of species interactions such as cross-feeding is uncertain. All the species can be cultured individually in uniform laboratory conditions, have reference genomes and have been phenotyped for various traits. These include the model disturbance for this study, streptomycin, with community members displaying a wide range of intrinsic susceptibility levels (Fig. 2a).

Pre-exposure of three abundant community members as monocultures to increasing levels of streptomycin led to increased disturbance resistance for two of the species: *Aeromonas* and *Pseudomonas chlororaphis* (Fig. 2a; *t*-tests on half-maximal inhibitory concentration (IC<sub>50</sub>) values of ancestral versus pre-exposed populations with

Bonferroni correction,  $P < 0.001$ ; Supplementary Table 1). In turn, the species *Citrobacter* was already intrinsically resistant before pre-exposure (Fig. 2a).

Whole-genome sequence data for pre-exposed populations of the 23 species supported trait evolutionary change (Fig. 2b). The predominant target of recurrent non-synonymous mutations reaching fixation or high allele frequency was the gene *rpsL*, encoding the streptomycin binding site in the small subunit of the ribosome, a known target of high-level streptomycin-resistance mutations<sup>27,28</sup>. These were also observed in two of the three abundant species used in the pre-exposure treatments: *Aeromonas* and *P. chlororaphis*. Moreover, recurrent mutations occurred in *rsmG* previously associated with low-level streptomycin resistance<sup>29</sup>.

One of the abundant species used in the pre-exposure treatment, *Citrobacter*, lacked mutations in *rpsL*, consistent with its intrinsic resistance and lacking the selection pressure to evolve de novo resistance (Fig. 2a). Its phenotypic resistance is supported by genomic data, as it contains four genes (*APH(3')-Ib*, *APH(6)-Id*, *strA* and *strB*) encoding aminoglycoside (including streptomycin) inactivating enzymes and seven genes (*acrD*, *baeR*, *baeS*, *cpxA*, *cpxR*, *kdpE* and *tolC*) encoding aminoglycoside efflux pumps<sup>25</sup>. Nevertheless, the pre-exposed population of *Citrobacter* did contain one low-frequency (7.5%) mutation in the multidrug efflux encoding gene *oprM*<sup>30</sup>. In addition, there could be mutations such as structural variants that were not detected because of the use of short-read sequencing data.

### Stronger disturbance led to stronger community change

In this study, we examine system change through changes in species abundance (relative abundance which is also a proxy for biomass), including alpha (within-community) diversity and beta (between-community) diversity. We examine alpha diversity through species richness and Shannon diversity, incorporating both species richness and evenness. We examine beta diversity, as previously<sup>16</sup>, through Kullback–Leibler (KL) divergence, which measures the relative entropy between two distributions (here, relative abundance vectors of communities) assuming values between 0 (perfect match) and  $\infty$ . KL divergence is more sensitive to small compositional changes at low abundances than Manhattan-based (for example, Bray–Curtis dissimilarity) and Euclidean-based measures<sup>31</sup>.

In the absence of dispersal, across the different pre-exposure histories, stronger disturbance led to a stronger change in community composition relative to the disturbance-free condition (permutational multivariate analysis of variance (PERMANOVA) model on community composition excluding community mixing treatments: disturbance level  $r^2 = 0.42$ ,  $P = 0.01$ , pairwise comparisons for streptomycin level all  $P < 0.04$ ; Supplementary Table 2; community composition in the different treatments is visualized in Fig. 3 top rows and Extended Data Figs. 1–3). In the presence of streptomycin, most species decreased in abundance but some species with higher resistance level increased in abundance (Fig. 3c top row; Extended Data Figs. 3 and 4; linear model for relationship between intrinsic resistance level and change in frequency in the absence of streptomycin pre-exposure or community mixing: coefficient of determination  $R^2 \approx 0.25$  and  $P < 0.001$  for both low and high streptomycin levels). These frequency changes approximate changes in absolute abundance owing to relatively constant community biomass levels in our experiment (Extended Data Figs. 5 and 6). Consistent with resistant cells being favoured with streptomycin, in the absence of dispersal, streptomycin level explained most of the variation (68.0%) in the IC<sub>50</sub> values of eight clones isolated at random from each experimental end-point community (Extended Data Fig. 7 and Supplementary Tables 3–6).

Streptomycin level also influenced community diversity. Higher Shannon diversity occurred at low streptomycin level compared to no streptomycin or high level (least diversity; Extended Data Fig. 8 and Supplementary Table 7). This was strongly influenced by the dominant

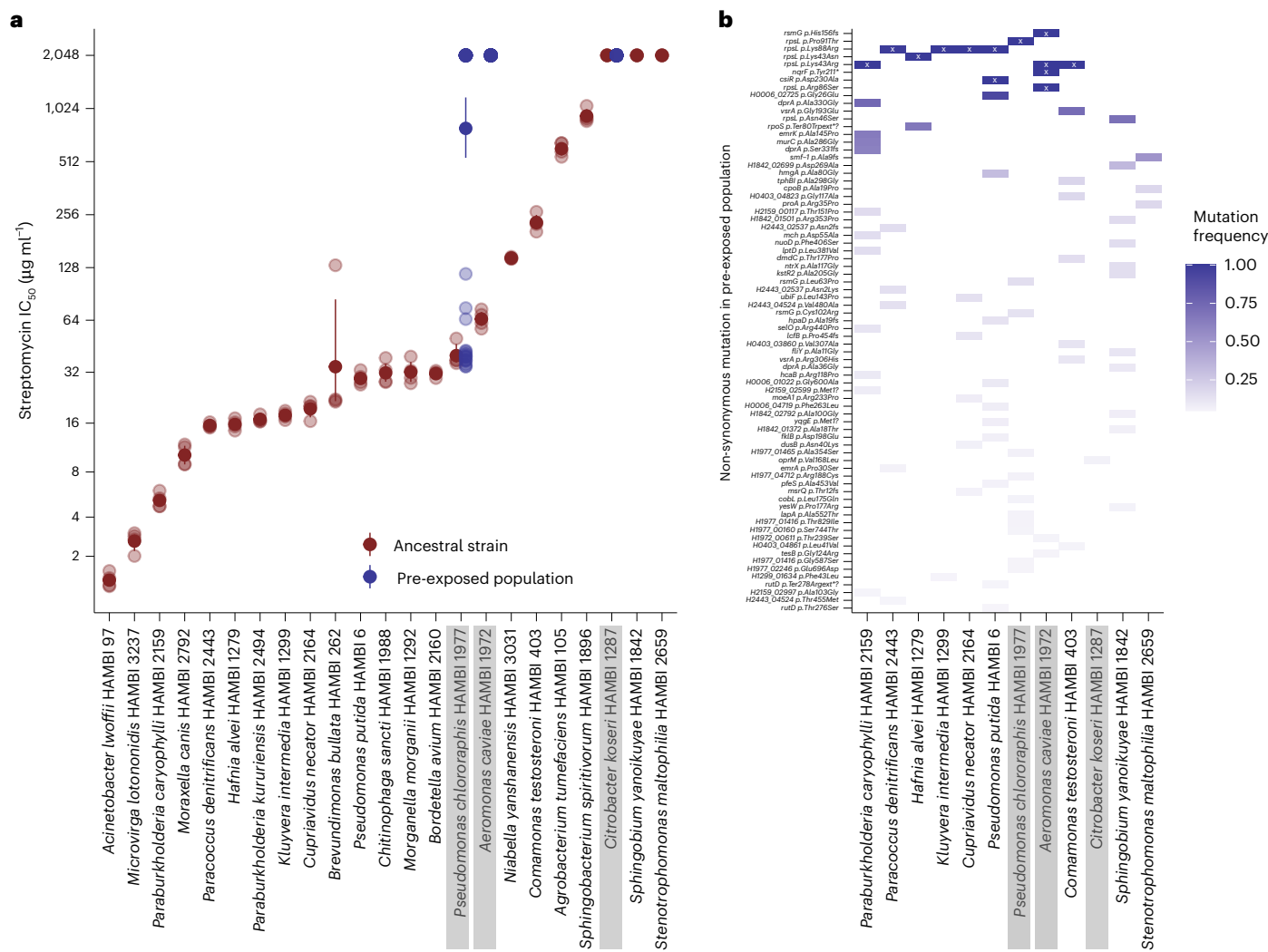


**Fig. 2 | Streptomycin susceptibility of experimental species and non-synonymous mutations in pre-exposed species. a**, Streptomycin susceptibility ( $IC_{50}$ ) for 23 experimental species. Four distinct clones from the ancestral species were phenotyped (transparent points) and are shown with the mean (muted red) and a non-parametric bootstrap for 95% confidence limits of the population mean (line range) across those replicate clones. Streptomycin  $IC_{50}$  of pre-exposed populations (muted blue) are shown for the three abundant species (axis labels highlighted with grey) in the community used in the pre-exposure treatment of the community experiment. For these, 16 clones were randomly phenotyped

from each of the four biological replicates for populations of each species following exposure to increasing concentrations of streptomycin (64 clones in total). **b**, Genes hit by non-synonymous mutations (single nucleotide polymorphisms or indels) at minimum 5% allele frequency in pre-exposed populations. In addition to the gene, the amino acid change is indicated in the y axis label. The streptomycin-resistance-associated genes *rpsL* and *rsmG* are highlighted with grey background. Fixed or near-fixed mutations (allele frequency minimum 0.95) are indicated with a white cross.

species *Aeromonas* whose population collapsed with streptomycin. This increased evenness at low streptomycin level, while high streptomycin level expectedly decreased diversity by driving species extinctions and competitive dominance of particular resistant species. This finding is consistent with the intermediate disturbance hypothesis positing that increasing disturbance levels initially increase diversity by reducing the abundance of competitively dominant species<sup>32</sup>. Nevertheless, the effect only holds for the *Aeromonas* species, as its pre-exposure to streptomycin removes the effect (Extended Data Fig. 8). Similarly, the effect was removed when all species were pre-exposed to streptomycin, without Shannon diversity reduction even at high disturbance level. Species richness alone showed a gradual drop at increasing streptomycin level with the extinction of susceptible species (Extended Data Fig. 9 and Supplementary Table 8). Similar to its effect on Shannon diversity, in the presence of streptomycin, pre-exposure of all species in the community maintained species richness.

**Pre-exposure decreased impact of disturbance on community**  
Although streptomycin drove most of the variation in community composition, pre-exposing community members to streptomycin itself also had a minor effect on composition (Extended Data Figs. 1, 2 and 10 and Supplementary Table 9). Since this study focuses on streptomycin as a model disturbance, pre-exposure was not treated as a disturbance. Instead, to control for the effect of pre-exposure, community data were examined relative to the streptomycin-free composition within each pre-exposure treatment.

Pre-exposure led to maintaining the abundance of more susceptible species that otherwise declined (Supplementary Fig. 1; analysis of variance (ANOVA) for linear model on frequency change of focal species in the absence of community mixing: streptomycin level  $F_{2,54} = 238.4$ ,  $P < 0.001$ ; absence/presence of pre-exposure  $F_{1,54} = 1,778$ ,  $P < 0.001$ ; species  $F_{2,54} = 1,195$ ; all interactions  $P < 0.001$ ; Supplementary Table 10). Without pre-exposure, the population of only one relatively susceptible species (Fig. 2a), *Aeromonas*, collapsed at low streptomycin level.



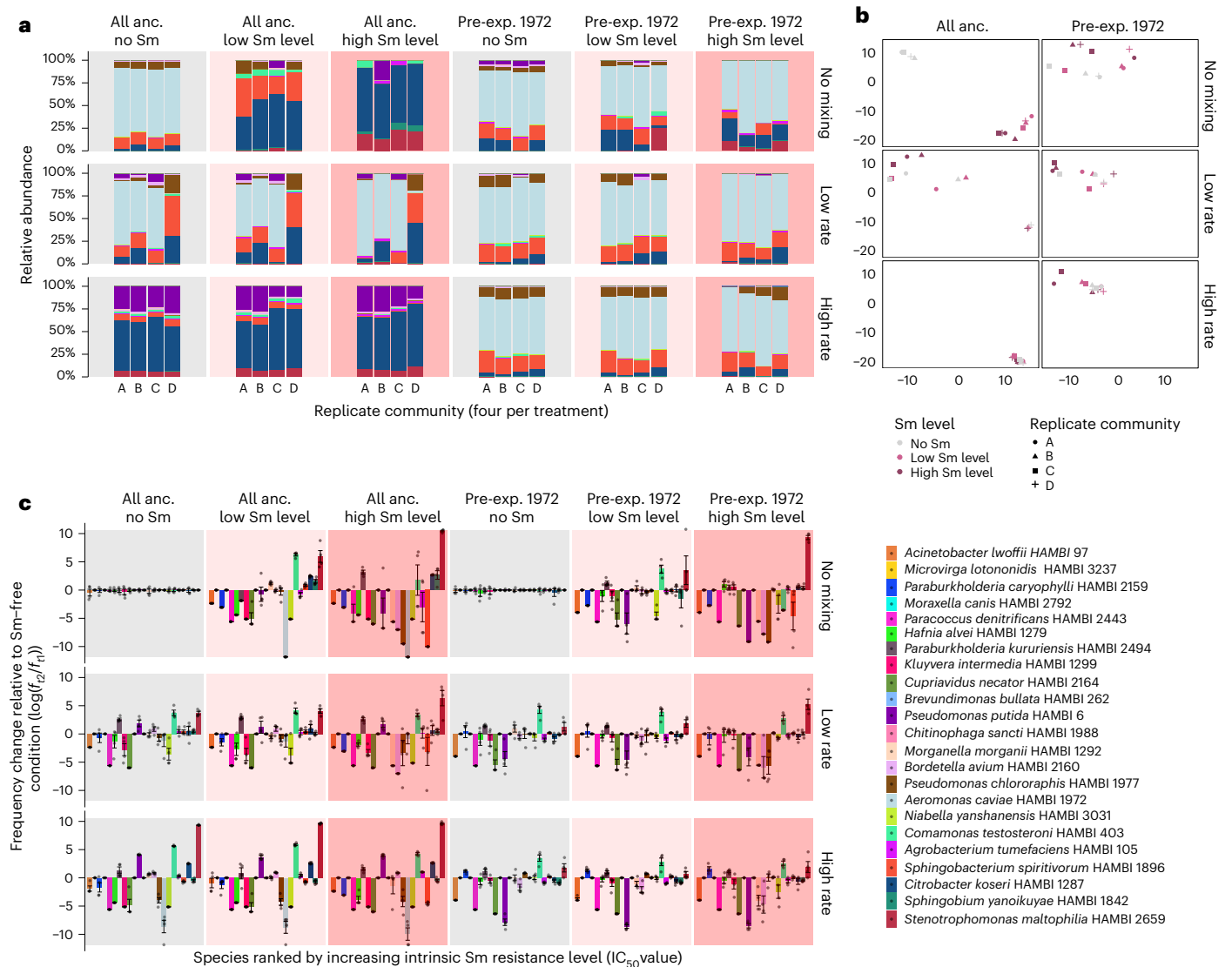


**Fig. 3 | Effect of disturbance, community mixing and pre-exposure of single most abundant community member (*Aeromonas caviae* HAMB1 1972) on community composition and disturbance resistance. **a**, Relative abundance of species at the end point of 46-day serial passage experiment ( $n = 4$  replicates per unique treatment combination). Subcolumns show data for the three disturbance levels (no, low or high streptomycin or Sm, level; deepening shades of red) in two key pre-exposure treatments, separated by black vertical lines from left to right as follows: (1) ancestral populations used for all species ('All anc. '); (2) a population used for the most abundant species in the undisturbed community, *A. caviae* HAMB1 1972, that had evolved to be highly resistant to the disturbance as a result of pre-exposure ('Pre-exp. 1972'). A model bacterial community consisting of 23 Gram-negative species was used in the experiment. The three streptomycin disturbance patches (no, low or high level) mixed at low or high rate have a shared history and can be identified by the replicate number shown on the x axis. **b**, A *t*-SNE map showing de novo community clustering at the end**

point of serial passage experiment. All data points originate from the same *t*-SNE analysis and have been separated into panels (with same arbitrary axis units) to illustrate how experimental treatments influence compositional divergence. The *t*-SNE map is a two-dimensional projection of a manifold in high-dimensional space, and only the relationship between the points is meaningful, not point positioning, with the axes given in arbitrary units. **c**, Frequency of each species relative to the frequency of the same species in the pre-exposure history-specific control condition with no antibiotic or community mixing (upper left-hand white corner) at the end point of serial passage experiment. Data are presented as mean  $\pm$  s.e.m. ( $n = 4$  replicates for each treatment condition). The data points in the control condition (top row with white background) represent variation of the four control replicates around their mean (zero) and therefore deviate from zero. The species have been ordered by increasing streptomycin resistance level ( $IC_{50}$  value) of the ancestral species.

In turn, regardless of pre-exposure, the population of the intrinsically resistant species *Citrobacter* increased in the presence of streptomycin.

At the community level, pre-exposure of abundant susceptible species (*Aeromonas* and *P. chlororaphis*) caused a decrease in compositional change at high streptomycin level compared to the absence of pre-exposure (Fig. 4). This was caused by two factors. First, maintaining abundance of the focal species itself decreased total community change (Fig. 4a and Supplementary Fig. 2). Second, for three out of four replicate communities for the most abundant and relatively

susceptible *Aeromonas* species, the non-focal community fraction was also protected from change (Fig. 4b; Tukey's post hoc test for non-focal community: *Aeromonas* versus *P. chlororaphis*,  $P = 0.061$ ; *Aeromonas* versus *Citrobacter*,  $P = 0.042$ ; Supplementary Table 11). The same result was found for compositional (directional) change as for the magnitude of change, such that only for pre-exposed *Aeromonas*, composition in the non-focal community fraction was significantly altered compared to the absence of pre-exposure (PERMANOVA model on community composition in the control condition without mixing or

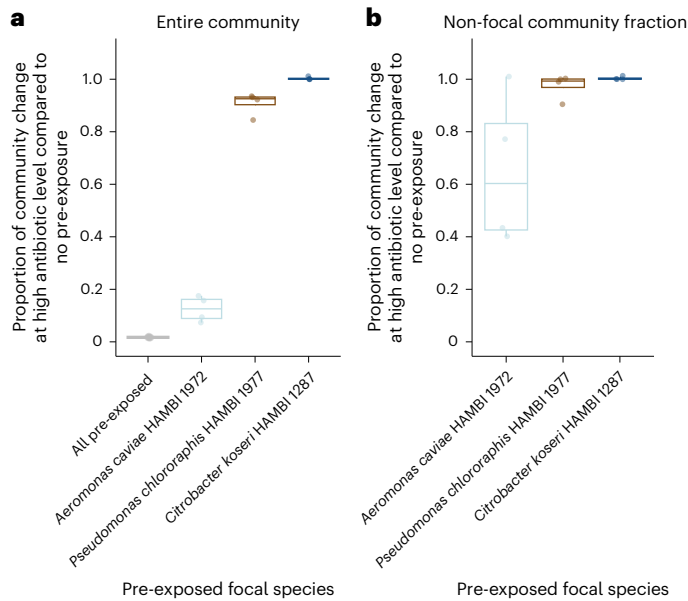


**Fig. 4 | Effect of streptomycin pre-exposure on community resilience.**

The y axis shows community resilience quantified as KL divergence of community composition from the streptomycin-free condition relative to the pre-exposure-free environment. Therefore, the lower the value, the less community change occurs at high streptomycin level and the more resilient the community is.

**a**, Resilience of the entire community at high streptomycin level. **b**, Resilience of the non-focal community fraction at high streptomycin level (that is, the pre-exposed species has been removed). Pre-exposed species have been ordered from left to right by increasing abundance in the control condition (antibiotic and pre-exposure-free environment), with the exception of placing the ‘all pre-exposed’ treatment in front of the list in **a** (absent from **b** as all community members have been pre-exposed). For both **a** and **b**, box plot bars and circles indicate medians and data points, respectively. The boxes indicate the interquartile range (25–75th percentile) and whiskers indicate lower and upper quartiles minus or plus 1.5 times the interquartile range.

streptomycin: *Citrobacter* pre-exposure  $r^2 = 0.12$ ,  $P = 0.40$ ; *Aeromonas* pre-exposure  $r^2 = 0.56$ ,  $P = 0.02$ ; *P. chlororaphis* pre-exposure  $r^2 = 0.18$ ,  $P = 0.30$ ; Supplementary Table 2). This effect includes, for example, better maintenance of *Hafnia alvei* and *Kluyvera intermedia* (Fig. 3c top right).

Since *Aeromonas* occupies up to 80% of the community without streptomycin, it is likely to strongly influence the resource environment. Its loss with streptomycin would represent a major additional disturbance, explaining why its maintenance with pre-exposure also protects certain other species from change. Consistent with this, at high streptomycin level without dispersal, the pre-exposure of *Aeromonas* led to the second lowest level of total community change after the pre-exposure of all community members (Supplementary Fig. 3; ANOVA for linear model on KL divergence of communities from pre-exposure treatment-specific baseline at experimental end point at high streptomycin level in the absence of community mixing: pre-exposure treatment  $F_{4,15} = 867$ ,  $P < 0.001$ ; Tukey’s post hoc test on all species pre-exposed versus other treatments and *Aeromonas* pre-exposed versus other treatments, all comparisons  $P < 0.001$ ; Supplementary Table 12).

### Dispersal spread patch features to metacommunity

As expected, dispersal spread patch features into the three-patch metacommunity (Fig. 3 and Extended Data Figs. 1–3). This caused intermediate species richness across the metacommunity when compared to the patches in the absence of dispersal, with Shannon diversity differences between the patches decreasing for most pre-exposure treatments from low to high dispersal rates (Extended Data Figs. 8

and 9 and Supplementary Tables 7 and 8). Consistent with this, dispersal spread streptomycin-resistant cells across the metacommunity from the high-streptomycin patch, such that the level of variation in  $IC_{50}$  values in clones isolated from the experimental end point explained by streptomycin in the individual patches decreased from 68.0% at no mixing through 26.6% at low mixing rate to 8.5% at high mixing rate (Extended Data Fig. 7 and Supplementary Tables 3–6). Therefore, consistent with theory, dispersal decreased metacommunity (beta) diversity (Supplementary Fig. 3; ANOVA for linear model on KL divergence of communities from pre-exposure treatment-specific baseline: community mixing rate  $F_{2,135} = 44.7$ ,  $P < 0.001$ ; community mixing rate  $\times$  streptomycin level  $F_{4,135} = 24.3$ ,  $P < 0.001$ ; community mixing rate  $\times$  pre-exposure treatment  $F_{8,135} = 25.0$ ,  $P < 0.001$ ; Tukey’s honestly significant difference for pairwise comparisons on community mixing rate, no mixing versus low/high mixing rate  $P < 0.001$ ; Supplementary Table 13).

To examine the effect of dispersal rate on resilience, we computed the mean composition of the communities across the three streptomycin levels for each pre-exposure treatment. This represents a null scenario where the dispersal treatment composition is simply the average of the composition in the three patches. We then tested whether community composition in the low or high dispersal rate treatments differed from this null scenario. If the composition significantly differs from the average composition at a particular dispersal rate, the dispersal rate disproportionately favours the spread of particular patch effects across the metacommunity rather than evenly homogenizing composition across the patches. In the absence of pre-exposure, the low dispersal rate corresponded to the null scenario whereas the high dispersal rate differed significantly from the null model and low dispersal rate (PERMANOVA model for all ancestral community: dispersal rate  $r^2 = 0.63$ ,  $P = 0.01$ ; pairwise comparisons: null model versus low  $P = 0.228$ , null versus high  $P = 0.003$ , low versus high  $P = 0.003$ ; Supplementary Table 2). This corresponded to a high magnitude of change from the streptomycin- and dispersal-free baseline community at high dispersal rate, representing decreased resilience at high compared to low mixing rate (Fig. 5a left; ANOVA for linear model on KL divergence of communities from the streptomycin- and dispersal-free condition: dispersal rate  $F_{1,44} = 78.2$ ,  $P < 0.001$ ; Supplementary Table 14). When comparing against the other dispersal-free patches, the dispersal rate leads all patches closer to the high streptomycin scenario (Fig. 3b, left). This also applied to some individual replicates within the low dispersal rate communities, seen as heightened variance between replicates with low dispersal rate, suggesting that the low dispersal rate used in this study was close to a community tipping point (Fig. 5b; ANOVA for linear model on effect of streptomycin disturbance and dispersal on variance between replicate communities: dispersal rate  $F_{2,36} = 6.1$ ,  $P = 0.005$ ; Tukey’s post hoc test for low versus no/high dispersal rate both  $P = 0.02$ , no versus high  $P = 1.0$ ; Supplementary Table 15).

### Pre-exposure removed dispersal–resilience relationship

Protection of the community through pre-exposure removed the negative association between dispersal rate and resilience (results shown for *Aeromonas* in Fig. 5a and Supplementary Fig. 3). For the pre-exposure of the dominant *Aeromonas caviae* species or all species, this was seen as only minor community change at low dispersal rate compared to the baseline (Supplementary Fig. 3) as well as lack of compositional difference between the low and high dispersal rate treatments (PERMANOVA model for *Aeromonas*: dispersal rate  $r^2 = 0.31$ ,  $P = 0.01$ ; pairwise comparisons: null model versus low  $P = 0.009$ , null versus high  $P = 0.003$ , low versus high  $P = 0.249$ ; PERMANOVA model for all pre-exposed: dispersal rate  $r^2 = 0.23$ ,  $P = 0.02$ ; pairwise comparisons: null model versus low  $P = 0.192$ , null versus high  $P = 0.033$ , low versus high  $P = 0.194$ ; Supplementary Table 2). Therefore, pre-exposure of *Aeromonas* or all species avoided spread of the streptomycin scenario across the metacommunity at high dispersal rate (for *Aeromonas*, see

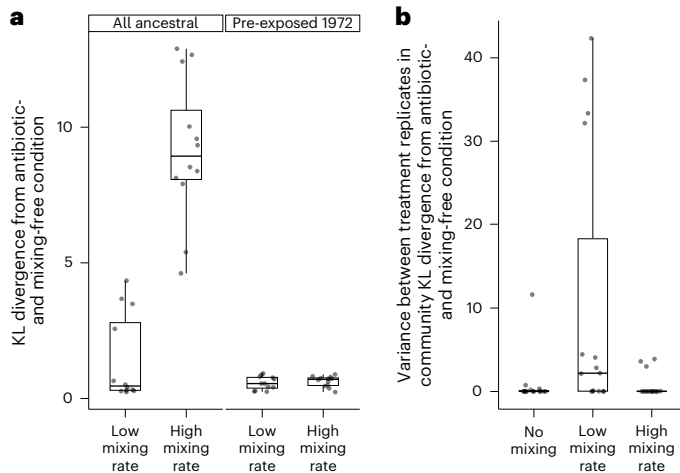


**Fig. 5 | Effect of community mixing rate and disturbance pre-exposure on resilience across metacommunities.** **a**, KL divergence from the streptomycin- and mixing-free environment at low and high community mixing rate for communities containing only ancestral species (left) and communities where the most dominant community member *A. caviae* HAMB1972 had been pre-exposed to streptomycin (right). Metacommunity refers to the three disturbance level patches (no, low or high streptomycin level) subject to community mixing. The 12 points overlaid above each box plot include the four replicates from each of the three streptomycin patches (streptomycin-free, low level and high level) comprising metacommunities. Each point indicates the compositional distance (KL divergence on y axis) of an individual community within the metacommunity from the streptomycin- and mixing-free (that is, no metacommunity) control condition (mean of four replicates) at the experimental end point. **b**, Variance in KL divergence between replicate communities in each treatment at different community mixing rates ( $n = 180$  communities per four replicates = 45 replicate sets). The 45 points overlaid above each box plot show variation among the four replicate communities in identical conditions (one of three streptomycin levels and one of five pre-exposure treatments) for each of the three community mixing rates. The y axis shows variance in KL divergence quantified as in **a**, indicating the level of variation among replicates in community change from the baseline (no streptomycin or community mixing) as a function of community mixing rate. For both **a** and **b**, box plot bars and circles indicate medians and data points, respectively. The boxes indicate the interquartile range (25–75th percentile) and whiskers indicate lower and upper quartiles minus or plus 1.5 times the interquartile range.

Fig. 3b, right). For pre-exposed *Citrobacter* and *P. chlororaphis*, where some community change occurred at low mixing rate (Supplementary Fig. 3), this was seen as smaller compositional change from the baseline at high compared to low dispersal rate (Supplementary Fig. 3), with low dispersal rate composition being closer to the equal mixing ratio null model (PERMANOVA model for *Citrobacter*: community mixing rate  $r^2 = 0.31$ ,  $P = 0.01$ ; pairwise comparisons: null model versus low  $P = 1.00$ , null versus high  $P = 0.006$ , low versus high  $P = 0.030$ ; PERMANOVA model for *P. chlororaphis*: community mixing rate  $r^2 = 0.34$ ,  $P = 0.02$ ; pairwise comparisons: null model versus low  $P = 1.00$ , null versus high  $P = 0.009$ , low versus high  $P = 0.030$ ; Supplementary Table 2). Therefore, pre-exposure of abundant species can strongly influence the relationship between dispersal and resilience.

## Discussion

Here we tested how pre-exposure to disturbance and dispersal influence disturbance response in 23-species metacommunities. As predicted, pre-exposure caused trait evolution (Fig. 2), decreasing the effect of the disturbance on the disturbed communities<sup>9</sup> (Fig. 4) and thereby also on the metacommunity (Fig. 5a). Moreover, as expect, dispersal homogenized species composition and traits across the metacommunity, reducing beta diversity compared to lack of dispersal (Fig. 3a)<sup>14,18,21</sup>. Since the different patches experienced different levels of disturbance,

this resulted in decreased diversity in the undisturbed patch and increased diversity in the high-disturbance patch (Extended Data Figs. 8 and 9 and Supplementary Tables 7 and 8)<sup>16,22–24</sup>. In the absence of pre-exposure, higher dispersal rates facilitated spread of disturbance effects, decreasing metacommunity resilience (compare ref. 21.) but this was cancelled by pre-exposure of abundant community members (Fig. 5a). These results show that the dispersal–resilience relationship depends on dispersal rate, and that the relationship is critically altered by pre-exposure of important community members.

There are several limitations in the current study that warrant future investigation. First, the mechanism underlying the negative relationship between dispersal rate and community resilience is uncertain. It could, for instance, be caused by decreased recovery time for the undisturbed patch between dispersal events at high dispersal rate. As we only collected end-point data, future studies including sampling over time are needed to test this hypothesis. Second, we found that pre-exposure of the dominant *Aeromonas* species to disturbance altered the abundance of the other community members, protecting the community from change with disturbance, but the reason for this should be addressed by future studies. A focal species could alter community-wide species composition through competition for shared resources, altering the resource landscape for the other species or through species interactions such as producing useful or harmful metabolites<sup>33–35</sup>. Stress conditions may also change the nature of species interactions<sup>15,36–38</sup>.

Third, our decision to choose focal species for the pre-exposure treatments based on their abundance could have led to the oversight of important species. Although in our setup changes in the single dominant *Aeromonas* species explained most of the variance in all experimental outcomes, it has generally been established that low-abundance species can also be critical for community functioning, such as cross-feeding networks<sup>39</sup>. Therefore, in the future, compositional data should be complemented by functional data (for example, transcriptomic or metabolomic) to inspect how species loss and evolutionary change alters metabolic pathways.

Fourth, in our study setup, dispersal was modelled by mixing entire communities. The high magnitude of dispersal is likely to have influenced the study results. For instance, very low dispersal rates may lead to species-poor communities with vacant niches<sup>20,40</sup>, which was probably averted in the low dispersal rate treatment in this study owing to mixing entire communities. Future studies varying both the magnitude and rate of dispersal are required to better elucidate these dynamics. An advantage of mixing entire communities is that our results may have implications for extending existing community coalescence theory<sup>19,41,42</sup> to a dynamic temporal setting.

Fifth, we observed a strong capacity of pre-exposure, particularly for the most abundant and stress-susceptible pre-exposure community members, to decrease the effect of the disturbance, also cancelling the spread of disturbance across the metacommunity at high dispersal rate (Fig. 5a). This demonstrates the potential of rapid evolution to improve ecological resilience, including in a metacommunity setting. Notably, however, we designed our experimental setup to quantify the maximum potential of rapid evolution by pre-exposing the species to be highly stress resistant. Moreover, we pre-exposed the species by exposing them to increasing levels of stress. The capacity for rapidly evolvable species to evolve de novo stress resistance is likely to be constrained during sudden exposure to high-level disturbance and when nested in a multispecies community<sup>13</sup>. In a multispecies community, susceptible species can rapidly become outcompeted by intrinsically resistant species and have lower population sizes (potentially decreasing evolvability) compared to when cultured alone, and a community context has been shown to constrain adaptation<sup>43</sup>.

One reason for our setup, maximizing the impact of rapid evolution through pre-exposure to a high streptomycin concentration without a community context, was that we had previously failed to



observe a clear effect of rapid evolution on community dynamics when communities consisting of initially unevolved species were exposed to antibiotic pulses<sup>16</sup>. Similar to that study, de novo evolution of streptomycin resistance is also likely to have occurred in multiple species during our study, although we lack the phenotypic and genomic data to test this explicitly. Owing to these previous findings from the same community exposed to the same antibiotic for a similar duration, we consider it unlikely that de novo evolution would be important for the dynamics in this system. Nevertheless, we did find some signals potentially indicating a minor influence of de novo evolution on community dynamics. For instance, in individual replicate communities, certain species with low  $IC_{50}$  values (*Hafnia*, *Kluyvera* and *Paraburkholderia*) increased in frequency at high streptomycin level (Fig. 3c, top row). Moreover, in one non-pre-exposed replicate community (*D*, low mixing rate; Fig. 3c, middle left), the population of the relatively susceptible species *Aeromonas* did not collapse as in all other communities lacking its pre-exposure. These cases may indicate the influence of de novo resistance evolution causing evolutionary rescue of these species in individual communities. The relatively brief time frame of these studies is a limitation, since there is limited time for rare de novo resistance mutations occurring at different times in the experiment to increase to high allele frequency and exert community-wide impacts. This may explain why initial species characteristics seems to drive these systems, and future studies with longer time frames may show greater community consequences of de novo evolution.

Our findings are relevant for designing successful control interventions to improve ecological resilience in natural communities. When there is absence of pre-exposure or low potential for rapid evolutionary change, low levels of dispersal between disturbed and undisturbed patches may facilitate metacommunity resilience. Our previous study suggests that one-way immigration from an undisturbed patch (source) to a disturbed patch is ideal for resilience, but this may not always be achievable<sup>16</sup>. However, our findings in this study suggest that, with high levels of dispersal, there is a risk of spreading eco-evolutionary effects of disturbances across metacommunities (see also ref. 21). Nevertheless, when there is high potential for evolutionary change in response to the disturbance or if pre-exposed populations of abundant taxa are introduced into a community, rapid trait evolution can be harnessed to protect from the disturbance at both local (patch) and global (metacommunity) levels.

Exploiting these features of rapid evolution and dispersal could be an effective tool for promoting compositional resilience in species communities facing environmental change. Nevertheless, this approach is also accompanied by risks. Reduced within-species diversity<sup>16</sup> or pleiotropic effects of resistance mutations<sup>44,45</sup> in an evolved species may cause community-wide changes in composition (as observed here) and function or affect the viability and resilience of the evolved species. Exploiting evolution and connectivity may still be considered worthwhile, as it is increasingly acknowledged that control interventions to steer ecology and evolution virtually always carry associated costs due to the complexity of biological systems<sup>4,9</sup>. An optimal control strategy for a given eco-evolutionary system, including one seeking to improve resilience, is one that strikes a balance between the importance of achieving a particular target and the importance of minimizing associated costs.

## Methods

### Synthetic bacterial community and experimental evolution

All experiments used synthetic assemblages of 23 different soil-, water- and host-associated bacterial species (Supplementary Table 16). Before the main experiment, all 23 species were experimentally evolved in two steps to have a maximum range of potential phenotypic and genotypic diversity derived from streptomycin exposure, thereby mimicking natural communities containing a legacy of past disturbance exposure within genetically heterogeneous populations. In the

first high-resistance generation step, monocultures of each species were grown in sub-minimal inhibitory concentrations (sub-MICs) of streptomycin (MICs from ref. 25) in protease peptone yeast extract (PPY) medium for 24–72 h at 28 °C. Monocultures were then serially transferred (96-deep-well plates; 1,500  $\mu$ l of PPY; 3% transfer volume, 48 h transfer interval; 28 °C, shaking at 1,000 rpm) with streptomycin concentrations doubling every transfer. The transfer series was stopped when bacterial optical density (OD) fell below 0.1 OD units (Supplementary Table 16) and 1 ml of the previous culture was frozen in 30% glycerol. In the second diversity generation step, evolved populations and ancestral forms of each species were revived from –80 °C and precultured (6 ml of Reasoner's 2A medium, R2A; 28 °C; shaking at 50 rpm; 96 h in total), then mixed in an equal ratio and grown for 48 h in duplicate (96-deep-well plates; 1,500  $\mu$ l of PPY; 3% transfer volume; 28 °C; shaking at 1,000 rpm) at 12 different streptomycin concentrations (0, 1, 5, 10, 20, 50, 100, 200, 500, 1,000, 2,000 and 5,000  $\mu$ g ml<sup>-1</sup>). After this round of growth, 100  $\mu$ l from each streptomycin concentration was combined per species. Each evolved population was frozen in 40% glycerol for later experimental use.

### Serial passage experiment and measurements

The main experiment was initiated with bacterial mixtures manually assembled into five pre-exposure histories: only ancestral forms of the 23 species ('all ancestral'), 22 ancestral species plus one experimentally pre-exposed population from one of three abundant species (*Citrobacter koseri* HAMBI 1287, *A. caviae* HAMBI 1972 or *P. chlororaphis* HAMBI 1977) and experimentally pre-exposed populations of all 23 species ('all pre-exposed'). These bacterial mixtures were assembled by first reviving the ancestral form and the pre-exposed population of each species from –80 °C and preculturing them for 24 h in R2A (6 ml; 25 °C; 50 rpm). One millilitre from each preculture was combined into one of the five pre-exposure treatments above, briefly mixed by vortexing, and then divided into four parts. These four parts were then used as the four replicate inoculae per evolutionary history for the main experiment. The initial species compositions differed slightly between the pre-exposure treatments (Supplementary Fig. 4). Notably, the species *Brevundimonas bullata* HAMBI 262 and *Chitinophaga sancti* HAMBI 1988 were not present at detectable levels in the community stock used to initiate the all pre-exposed treatment. Among these species, *B. bullata* HAMBI 262 was detected in the all pre-exposed treatment at the experimental end point (Extended Data Fig. 1). *C. sancti* HAMBI 1988 was present in the other treatments at very low levels at the experimental end point, suggesting that its absence from the all pre-exposed treatments is unlikely to have influenced the findings in the study. Originally, the pre-exposure treatment also included the species *Pseudomonas putida* HAMBI 6, *Agrobacterium tumefaciens* HAMBI 105 and *Sphingobacterium spiritivorum* HAMBI 1896. However, whole-genome sequence analysis of the pre-exposed populations of these species used to initiate the serial passage experiment showed them to be contaminated with other pre-exposed species. They were therefore omitted from the analysis.

Next, three different streptomycin concentrations (0, 20 or 1,000  $\mu$ g ml<sup>-1</sup>) representing three levels of disturbance were applied to each replicate per evolutionary history. Finally, a community mixing treatment was nested within replicates of each evolutionary history to simulate differing amounts of connectivity between streptomycin 'patches'. In the no-mixing treatment, each streptomycin patch was serially transferred to the same streptomycin patch. In the low mixing rate treatment, the three streptomycin patches were thoroughly mixed every 12 days (six transfers), and this mixture was used to inoculate all streptomycin patches in the next transfer. The high mixing rate treatment was the same as the low mixing rate treatment, but mixing occurred every 6 days (three transfers). The mixing treatment consisted of mixing equal volumes of all three streptomycin levels (0, 20 and 100  $\mu$ g ml<sup>-1</sup>), resulting in a concentration in the mix of 353  $\mu$ g ml<sup>-1</sup>.



The protocol leads to a maximum streptomycin concentration of  $\sim 10 \mu\text{g ml}^{-1}$  (assuming no degradation of streptomycin during previous culture cycle) after the first transfer following mixing, and negligible amounts thereafter before the next mixing event (for example,  $0.3 \mu\text{g ml}^{-1}$  after second transfer). Such a residual streptomycin level may have imposed some selection in the streptomycin-free patch in the first culture cycle after community mixing, as it exceeds the  $\text{IC}_{50}$  value of three low-abundance species in the community (*Acinetobacter lwoffii* HAMBI 97, *Microvirga lotononidis* HAMBI 3237 and *Paraburkholderia caryophylli* HAMBI 2159; Fig. 2a). However, this residual level should not affect the competitive dynamics of the two dominant species *C. koseri* HAMBI 1287 (high-resistance) and *A. caviae* HAMBI 1972 (more susceptible), as the growth of the latter is not impaired until concentrations  $>16 \mu\text{g ml}^{-1}$  (Supplementary Fig. 5). Therefore, in the community mixing treatment, the dominance of either strain should be driven purely by density-dependent effects based on the intrinsic or evolved traits of the strains (growth and resistance) in the different streptomycin patches.

Experimental microcosms were maintained for 23 serial transfers (96-deep-well plates; 1,500  $\mu\text{l}$  of R2A; 3% transfer volume; 48 h transfer interval; 25 °C, shaking at 1,000 rpm) in the appropriate streptomycin concentration. For the low and high mixing rate treatments, 780  $\mu\text{l}$  from the three streptomycin concentrations were pooled, vortexed and used as the next inoculum in the series. Optical density (600 nm) was measured every 48 h (Extended Data Fig. 5). After the 23rd transfer, an aliquot was cryopreserved (40% glycerol) to be revived later for the dose–response analysis (see below). The remainder of each sample was destructively harvested to collect material for DNA extraction and amplicon sequencing.

### Sequencing and bioinformatics

Bulk DNA was extracted from a 500  $\mu\text{l}$  aliquot of experimental samples (cryopreserved in 40% glycerol) using the DNeasy 96 Blood & Tissue Kit (Qiagen) according to the manufacturer's instructions. The V3–V4 hypervariable region of the 16S ribosomal RNA gene was amplified from total community DNA following the standard Illumina 16S metagenomic sequencing library preparation protocol (Illumina). Briefly, the protocol uses the primer pair PCR1\_Forward (50 base pairs (bp)): 5'–TCGTCGGCAGCGTCAGATGTGTATAAGAGACAGCCTACGGGNG-GCWGCAG–3', PCR1\_Reverse (55 bp): 5'–GTCTCGTGGGCTCGGAGATGTGTATAAGAGACAGGACTACHVGGGTATCTAATCC–3' in a limited-cycle polymerase chain (PCR) reaction, then attaches Nextera XT barcodes using a dual-index arrangement. The libraries were then pooled and sequenced on an Illumina MiSeq using paired 300 bp reads and MiSeq v.3 reagents at the Finnish Institute of Molecular Medicine. Library indices were subsequently demultiplexed using bcl2fastq v.2.2. Paired-end 16S rRNA amplicon reads were then quality trimmed, merged, filtered and mapped to a reference of the 16S rRNA gene from the 23 species as previously described<sup>46</sup>. Before data analysis, species counts were normalized by species-specific 16S rRNA gene copy number.

Genomic DNA from ancestral forms and one replicate of the evolved populations was extracted using the DNeasy 96 Blood & Tissue Kit (Qiagen) from 24 h overnight cultures grown in PPY medium. Sequencing of genomic DNA was performed at SeqCenter (<https://www.seqcenter.com/>). Sample libraries were prepared using the Illumina DNA Prep kit and IDT 10 bp UDI indices and sequenced on an Illumina NextSeq 2000, producing  $2 \times 151$  bp reads. Demultiplexing, quality control and adaptor trimming were performed with bcl-convert (v.3.9.3).

To ensure that the pre-exposed starting populations were axenic, reads were competitively mapped against a set of closed reference genomes using bbsplit (<https://sourceforge.net/projects/bbmap/>). This tool simultaneously maps reads against several reference genomes and identifies the best-matching genome for each read pair.

We excluded all read pairs mapping ambiguously to more than one reference genome (that is, multiple mapping positions within a containment threshold of the top-scoring mapping position) but kept reads that mapped ambiguously within a single genome. Starting populations with significant contamination from other species were discarded from further analysis. The purity of the starting populations was then verified via PCR of the 16S rRNA gene (primers 27 F and 1492 R) and Sanger sequencing, to ensure that only one template was present in the sequencing reaction. Sanger sequencing traces of all replicates of *C. koseri* 1287, *A. caviae* 1972 and *P. chlororaphis* 1977 did not have multiple peaks at any position, confirming the taxonomic purity from competitive read mapping.

The competitive mapping process generated a set of read pairs unique to the expected species from each experimentally evolved population. Evolved species with  $<25\times$  coverage of the target genome (HAMBI 97, 105, 262, 1988 and 3237; Supplementary Table 16) were excluded from downstream analysis. Taxonomically verified read pairs were mapped to closed reference genomes for each species<sup>47</sup> using BWA-mem v.0.7.17 (ref. 48). Alignment files were preprocessed with GATK v.4.4 following best practices<sup>49</sup>. Mutect2 from GATK v.4.4 (ref. 50) was used to call genomic variants using default parameters, and mutect calls were filtered to exclude spurious calls using FilterMutectCalls with the --microbial-mode option. Filtered variants were annotated using SnpEff v.4.3 (ref. 51). Gene calls were from Prokka v.1.14.6 (ref. 52). Functional annotations of genes were derived from the Prokka internal database and the eggNOG 6.0 database<sup>53</sup> using eggNOG-mapper v.2.1.10 (ref. 53).

### Inference of $\text{IC}_{50}$ values

Using a dose–response curve analysis, half-maximal inhibitory streptomycin concentrations ( $\text{IC}_{50}$ ) were estimated for the ancestral forms of each bacterial species, the pre-exposed populations of the three abundant species used in the pre-exposure treatment (*C. koseri* HAMBI 1287, *A. caviae* HAMBI 1972 and *P. chlororaphis* HAMBI 1977) and for clones randomly picked from the final time point in the experiment. Clones of ancestral/evolved forms of each species and from the experiment end point (day 46) were picked from agar plates and precultured for 24 h in PPY medium, then inoculated at a density of 0.01  $\text{OD}_{600}$  into 200  $\mu\text{l}$  of R2A medium at streptomycin concentrations of 0, 1, 2, 4, 8, 16, 32, 64, 128, 256, 512, 1,024, 2,048, 4,096 and 8,192  $\mu\text{g ml}^{-1}$ . Cultures were grown for 48 h at 25 °C in 96-well plates with shaking (1,000 rpm) and culture density was assessed at 48 h using  $\text{OD}_{600}$ . For the strains used to initiate the experiment, four replicate dose–response experiments were performed for each ancestral species (four clones per species) and 64 for each population of the three pre-exposed species. For the experimental end-point communities, eight clones were isolated and tested from each of the 180 communities (1,440 clones in total).

Dose–response curves were fit to the resulting blank-corrected optical density data from each species or clone following ref. 54 but using a four-parameter log-logistic function of the form

$$f(x) = c + \frac{d - c}{1 + \exp(b(\log(x) - \log(e)))}$$

where  $c$  is the lower asymptote,  $d$  is the upper asymptote,  $b$  is the slope at the inflection point and  $e$  is the  $\text{IC}_{50}$  value or the antibiotic concentration where the growth (optical density) is at half the maximum value. The log-logistic function was fit to the optical density measurements using the Levenberg–Marquardt nonlinear least-squares algorithm implemented in minpack.lm v.1.2-4 in R v.4.2.2.  $\text{IC}_{50}$  values were set to the maximum tested streptomycin concentration when optical density was always  $>0.2 \text{OD}_{600}$  units and did not decrease across the assayed streptomycin concentration range in a sigmoid shape with a clearly defined upper and lower asymptote.

### Downstream data analyses

All downstream analyses were performed in the R v.4.2.3 environment<sup>55</sup>. The *t*-distributed stochastic neighbour embedding (*t*-SNE) map for Fig. 3b and Extended Data Fig. 2 was created using the Rtsne package<sup>56</sup> with the options perplexity = 20 and theta = 0.5. PERMANOVA<sup>57</sup> as implemented in the *adonis* function in the *vegan* package<sup>58</sup> was used to test whether the antibiotic level, community mixing rate or pre-exposure treatment affected community composition. The method tests the probability that the observed distances between groups could arise by chance by comparing them with random permutations of the raw data<sup>59</sup>. The influence of the experimental treatments on IC<sub>50</sub> and KL divergence values relative to the pre-exposure history-specific baseline (streptomycin- and mixing-free condition) was investigated using linear regression models.

### Reporting summary

Further information on research design is available in the Nature Portfolio Reporting Summary linked to this article.

### Data availability

Raw sequence data (fastq files) have been deposited in the NCBI Sequence Read Archive under the accession PRJNA1126612. Pre-processed data on the growth of pre-exposed species at different streptomycin concentrations, genomic variants of pre-exposed species, community size in the main experiment and community composition in the main experiment are available via Zenodo at <https://doi.org/10.5281/zenodo.14015860.60> (ref. 60).

### Code availability

All code needed to reproduce the downstream analyses and figures are available via Zenodo at <https://doi.org/10.5281/zenodo.14015860> (ref. 60).

### References

- Rykiel, E. J. Towards a definition of ecological disturbance. *Aust. J. Ecol.* **10**, 361–365 (1985).
- Bender, E. A., Case, T. J. & Gilpin, M. E. Perturbation experiments in community ecology: theory and practice. *Ecology* **65**, 1–13 (1984).
- Shade, A. et al. Fundamentals of microbial community resistance and resilience. *Front. Microbiol.* **3**, 417 (2012).
- Lässig, M., Mustonen, V. & Nourmohammad, A. Steering and controlling evolution—from bioengineering to fighting pathogens. *Nat. Rev. Genet.* **24**, 851–867 (2023).
- Pimm, S. L. The complexity and stability of ecosystems. *Nature* **307**, 321–326 (1984).
- Holling, C. S. Resilience and stability of ecological systems. *Annu. Rev. Ecol. Syst.* **4**, 1–23 (1973).
- Scheffer, M. et al. Anticipating critical transitions. *Science* **338**, 344–348 (2012).
- Dakos, V. et al. Ecosystem tipping points in an evolving world. *Nat. Ecol. Evol.* **3**, 355–362 (2018).
- Thorogood, R. et al. Understanding and applying biological resilience, from genes to ecosystems. *npj Biodivers.* **2**, 16 (2023).
- Barnosky, A. D. et al. Approaching a state shift in Earth's biosphere. *Nature* **486**, 52–58 (2012).
- Buckling, A., Craig Maclean, R., Brockhurst, M. A. & Colegrave, N. The beagle in a bottle. *Nature* **457**, 824–829 (2009).
- Bottery, M. J., Pitchford, J. W. & Friman, V.-P. Ecology and evolution of antimicrobial resistance in bacterial communities. *ISME J.* **15**, 939–948 (2020).
- Klümper, U. et al. Selection for antimicrobial resistance is reduced when embedded in a natural microbial community. *ISME J.* **13**, 2927–2937 (2019).
- O'Connor, L. M., Fugère, V. & Gonzalez, A. Evolutionary rescue is mediated by the history of selection and dispersal in diversifying metacommunities. *Front. Ecol. Evol.* **8**, 517434 (2020).
- Pathak, A., Angst, D. C., León-Sampedro, R. & Hall, A. R. Antibiotic-degrading resistance changes bacterial community structure via species-specific responses. *ISME J.* **17**, 1495–1503 (2023).
- Cairns, J., Jokela, R., Becks, L., Mustonen, V. & Hiltunen, T. Repeatable ecological dynamics govern the response of experimental communities to antibiotic pulse perturbation. *Nat. Ecol. Evol.* **4**, 1385–1394 (2020).
- Thompson, P. L. et al. A process-based metacommunity framework linking local and regional scale community ecology. *Ecol. Lett.* **23**, 1314–1329 (2020).
- Loke, L. H. & Chisholm, R. A. Unveiling the transition from niche to dispersal assembly in ecology. *Nature* **618**, 537–542 (2023).
- Castledine, M., Sierocinski, P., Padfield, D. & Buckling, A. Community coalescence: an eco-evolutionary perspective. *Philos. Trans. R. Soc. B* **375**, 20190252 (2020).
- Mouquet, N. & Loreau, M. Community patterns in source-sink metacommunities. *Am. Nat.* **162**, 544–557 (2003).
- Pearson, R. M. et al. Disturbance type determines how connectivity shapes ecosystem resilience. *Sci. Rep.* **11**, 1188 (2021).
- Heinrichs, J. A., Lawler, J. J. & Schumaker, N. H. Intrinsic and extrinsic drivers of source-sink dynamics. *Ecol. Evol.* **6**, 892–904 (2016).
- Larsson, D. G. & Flach, C.-F. Antibiotic resistance in the environment. *Nat. Rev. Microbiol.* **20**, 257–269 (2021).
- Heß, S. et al. Sewage from airplanes exhibits high abundance and diversity of antibiotic resistance genes. *Environ. Sci. Technol.* **53**, 13898–13905 (2019).
- Cairns, J. et al. Construction and characterization of synthetic bacterial community for experimental ecology and evolution. *Front. Genet.* **9**, 312 (2018).
- Hogle, S. L., Ruusulehto, L., Cairns, J., Hultman, J. & Hiltunen, T. Localized coevolution between microbial predator and prey alters community-wide gene expression and ecosystem function. *ISME J.* **17**, 514–524 (2023).
- Pelchovich, G., Schreiber, R., Zhuravlev, A. & Gophna, U. The contribution of common *rpsL* mutations in *Escherichia coli* to sensitivity to ribosome targeting antibiotics. *Int. J. Med. Microbiol.* **303**, 558–562 (2013).
- Finken, M., Kirschner, P., Meier, A., Wrede, A. & Böttger, E. C. Molecular basis of streptomycin resistance in *Mycobacterium tuberculosis*: alterations of the ribosomal protein S12 gene and point mutations within a functional 16S ribosomal RNA pseudoknot. *Mol. Microbiol.* **9**, 1239–1246 (1993).
- Nishimura, K., Hosaka, T., Tokuyama, S., Okamoto, S. & Ochi, K. Mutations in *rsmG*, encoding a 16S rRNA methyltransferase, result in low-level streptomycin resistance and antibiotic overproduction in *Streptomyces coelicolor* A3(2). *J. Bacteriol.* **189**, 3876–3883 (2007).
- Bianco, N., Neshat, S. & Poole, K. Conservation of the multidrug resistance efflux gene *oprM* in *Pseudomonas aeruginosa*. *Antimicrob. Agents Chemother.* **41**, 853–856 (1997).
- Chen, B., He, X., Pan, B., Zou, X. & You, N. Comparison of beta diversity measures in clustering the high-dimensional microbial data. *PLoS ONE* **16**, e0246893 (2021).
- Connell, J. H. Diversity in tropical rain forests and coral reefs. *Science* **199**, 1302–1310 (1978).
- Rodríguez-Verdugo, A. & Ackermann, M. Rapid evolution destabilizes species interactions in a fluctuating environment. *ISME J.* **15**, 450–460 (2020).
- Estrela, S., Trisos, C. H. & Brown, S. P. From metabolism to ecology: cross-feeding interactions shape the balance between polymicrobial conflict and mutualism. *Am. Nat.* **180**, 566–576 (2012).

35. Estrela, S. & Brown, S. P. Metabolic and demographic feedbacks shape the emergent spatial structure and function of microbial communities. *PLoS Comput. Biol.* **9**, e1003398 (2013).
36. Callaway, R. M. et al. Positive interactions among alpine plants increase with stress. *Nature* **417**, 844–848 (2002).
37. Cairns, J. et al. Black queen evolution and trophic interactions determine plasmid survival after the disruption of the conjugation network. *mSystems* **3**, e00104–e00118 (2018).
38. Davies, D. Understanding biofilm resistance to antibacterial agents. *Nat. Rev. Drug Discov.* **2**, 114–122 (2003).
39. Marcelino, V. R. et al. Disease-specific loss of microbial cross-feeding interactions in the human gut. *Nat. Commun.* **14**, 6546 (2023).
40. Declerck, S. A., Winter, C., Shurin, J. B., Suttle, C. A. & Matthews, B. Effects of patch connectivity and heterogeneity on metacommunity structure of planktonic bacteria and viruses. *ISME J.* **7**, 533–542 (2013).
41. Estrela, S. et al. Functional attractors in microbial community assembly. *Cell Syst.* **13**, 29–42 (2022).
42. Diaz-Colunga, J. et al. Top-down and bottom-up cohesiveness in microbial community coalescence. *Proc. Natl Acad. Sci. USA* **119**, e2111261119 (2022).
43. Scheuerl, T. et al. Bacterial adaptation is constrained in complex communities. *Nat. Commun.* **11**, 754 (2020).
44. Melnyk, A. H., Wong, A. & Kassen, R. The fitness costs of antibiotic resistance mutations. *Evol. Appl.* **8**, 273–283 (2014).
45. Ardell, S. M. & Kryazhimskiy, S. The population genetics of collateral resistance and sensitivity. *eLife* **10**, e73250 (2021).
46. Hogle, S. L., Hepolehto, I., Ruokolainen, L., Cairns, J. & Hiltunen, T. Effects of phenotypic variation on consumer coexistence and prey community structure. *Ecol. Lett.* **25**, 307–319 (2021).
47. Hogle, S. L., Tamminen, M. & Hiltunen, T. Complete genome sequences of 30 bacterial species from a synthetic community. *Microbiol. Resour. Announc.* **13**, e0011124 (2024).
48. Li, H. Aligning sequence reads, clone sequences and assembly contigs with BWA-MEM. Preprint at <https://doi.org/10.48550/arXiv.1303.3997> (2013).
49. Van der Auwera, G. A. *Genomics in the Cloud: Using Docker, GATK, and WDL in Terra* (O'Reilly Media, 2020).
50. Benjamin, D. T. S., Cibulskis, K., Getz, G., Stewart, C. & Lichtenstein, L. Calling somatic SNVs and indels with Mutect2. Preprint at *bioRxiv* <https://doi.org/10.1101/861054> (2019).
51. Cingolani, P. et al. A program for annotating and predicting the effects of single nucleotide polymorphisms, SnpEff. *Fly* **6**, 80–92 (2012).
52. Seemann, T. Prokka: rapid prokaryotic genome annotation. *Bioinformatics* **30**, 2068–2069 (2014).
53. Hernandez-Plaza, A. et al. eggNOG 6.0: enabling comparative genomics across 12 535 organisms. *Nucleic Acids Res.* **51**, D389–D394 (2023).
54. Sebaugh, J. L. Guidelines for accurate EC50/IC50 estimation. *Pharm. Stat.* **10**, 128–134 (2011).
55. R Core Team. *R: A Language and Environment for Statistical Computing* (R Foundation for Statistical Computing, 2023).
56. Krijthe, J. Rtsne: T-distributed stochastic neighbor embedding using a Barnes-Hut implementation. R package version 0.15. *GitHub* <https://github.com/jkrijthe/Rtsne> (2015).
57. Zapala, M. A. & Schork, N. J. Multivariate regression analysis of distance matrices for testing associations between gene expression patterns and related variables. *Proc. Natl Acad. Sci. USA* **103**, 19430–19435 (2006).
58. Oksanen, J. et al. *vegan: Community ecology package*. R package version 2.6-4 <https://CRAN.R-project.org/package=vegan> (2022).
59. Anderson, M. J. A new method for non-parametric multivariate analysis of variance. *Austral Ecol.* **26**, 32–46 (2001).
60. Cairns, J. Pre-exposure of abundant species to disturbance improves resilience in microbial metacommunities [Data set]. *Zenodo* <https://doi.org/10.5281/zenodo.14015860> (2024).

## Acknowledgements

We thank E. Liinoja and I.-M. Hyvönen for technical assistance. This work was funded by the Research Council of Finland (Multidisciplinary Center of Excellence in Antimicrobial Resistance Research, grant no. 346126; grant nos. 330886 and 327741 to T.H.; and grant no. 346128 to V.M.).

## Author contributions

T.H. and S.H. designed the serial passage experiment. E.A. performed the serial passage experiment. J.C., S.H. and V.M. designed the data analysis. J.C. and S.H. performed the data analysis. J.C., T.H., S.H. and V.M. were responsible for interpreting results. J.C. wrote the first paper draft, with contributions from all authors. All authors approved the final version of the paper.

## Competing interests

The authors declare no competing interests.

## Additional information

**Extended data** is available for this paper at <https://doi.org/10.1038/s41559-024-02624-0>.

**Supplementary information** The online version contains supplementary material available at <https://doi.org/10.1038/s41559-024-02624-0>.

**Correspondence and requests for materials** should be addressed to Teppo Hiltunen.

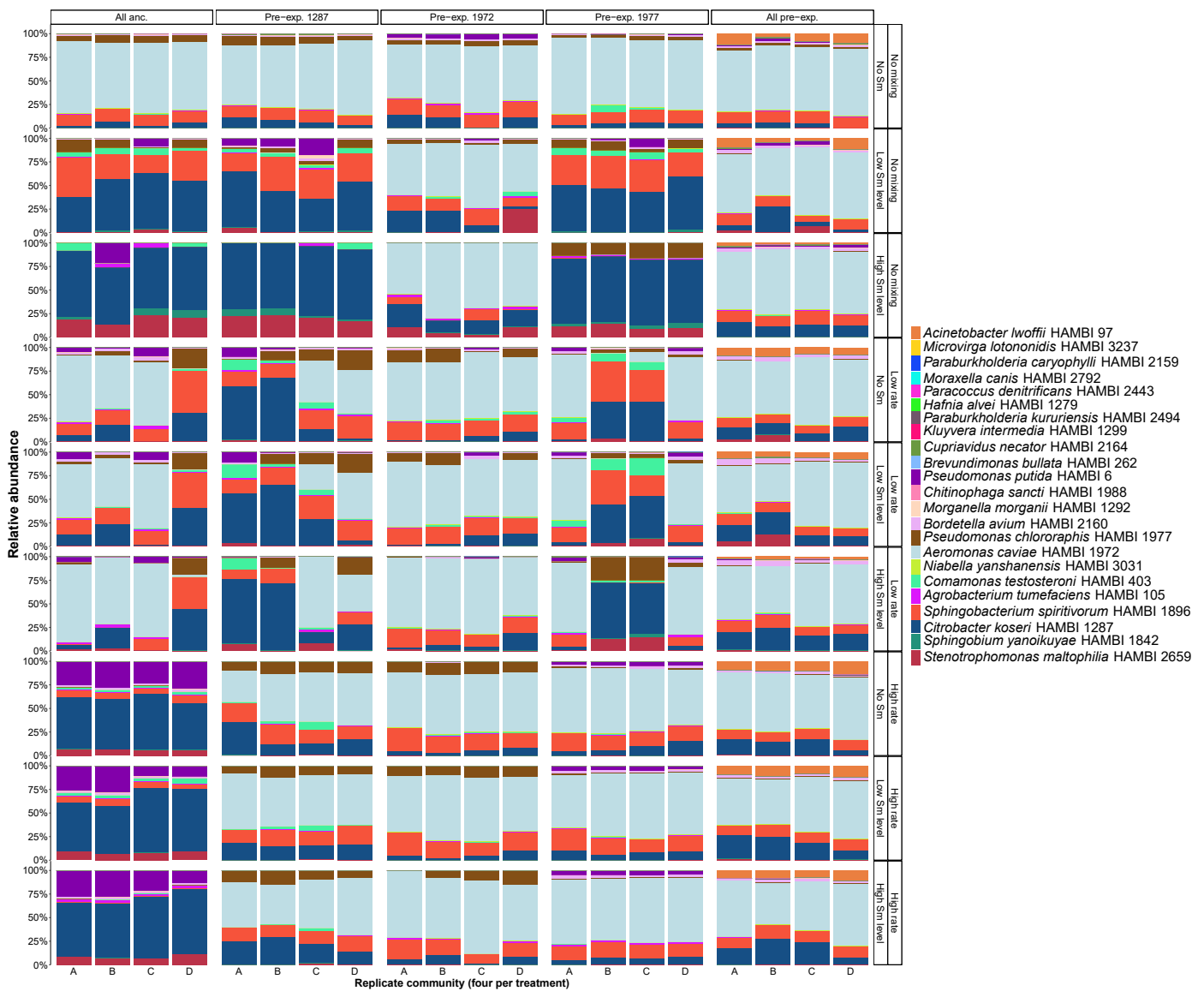
**Peer review information** *Nature Ecology & Evolution* thanks Massimo Amicone, Olivia Kosterlitz, Sara Mitri and the other, anonymous, reviewer(s) for their contribution to the peer review of this work.

**Reprints and permissions information** is available at [www.nature.com/reprints](http://www.nature.com/reprints).

**Publisher's note** Springer Nature remains neutral with regard to jurisdictional claims in published maps and institutional affiliations.

Springer Nature or its licensor (e.g. a society or other partner) holds exclusive rights to this article under a publishing agreement with the author(s) or other rightsholder(s); author self-archiving of the accepted manuscript version of this article is solely governed by the terms of such publishing agreement and applicable law.

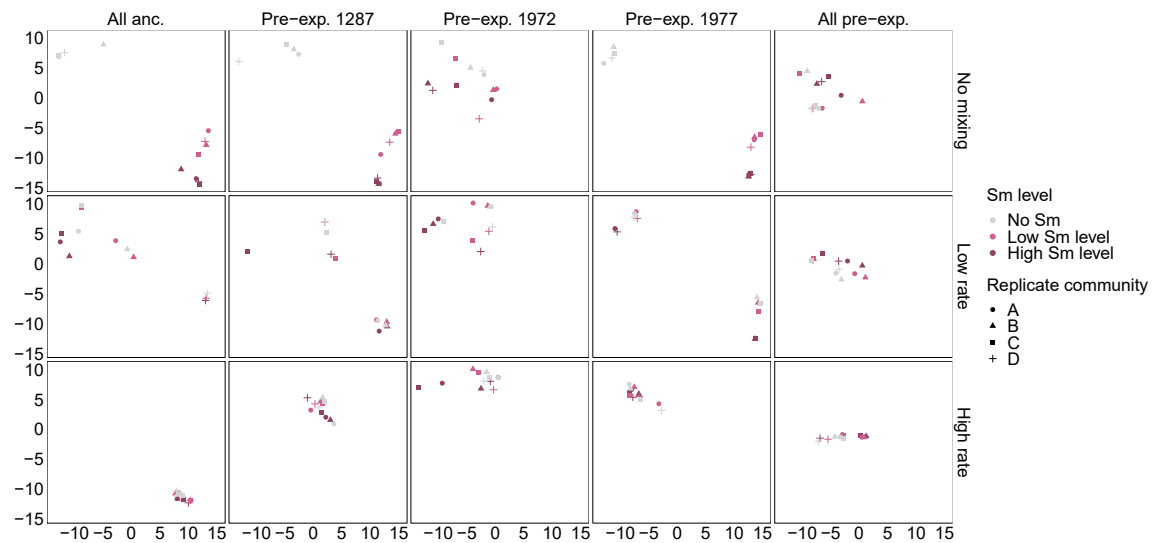
© The Author(s), under exclusive licence to Springer Nature Limited 2025



**Extended Data Fig. 1 | Effect of disturbance, community mixing and pre-exposure on community composition.** Relative abundance of species (normalized by species-specific 16S rRNA gene copy number) at the end-point of 46-day serial passage experiment ( $N = 4$  replicates per unique treatment combination). Subcolumns show data for the five pre-exposure treatments from left to right as follows: (1) ancestral strains used for all species ('All anc. '); (2–4) a population used for one of three abundant species that had been pre-exposed to the disturbance ('Pre-exp. '); HAMB1 Culture Collection code indicated in column label: *Citrobacter koseri* HAMB1 1287, *Aeromonas caviae* HAMB1 1972,

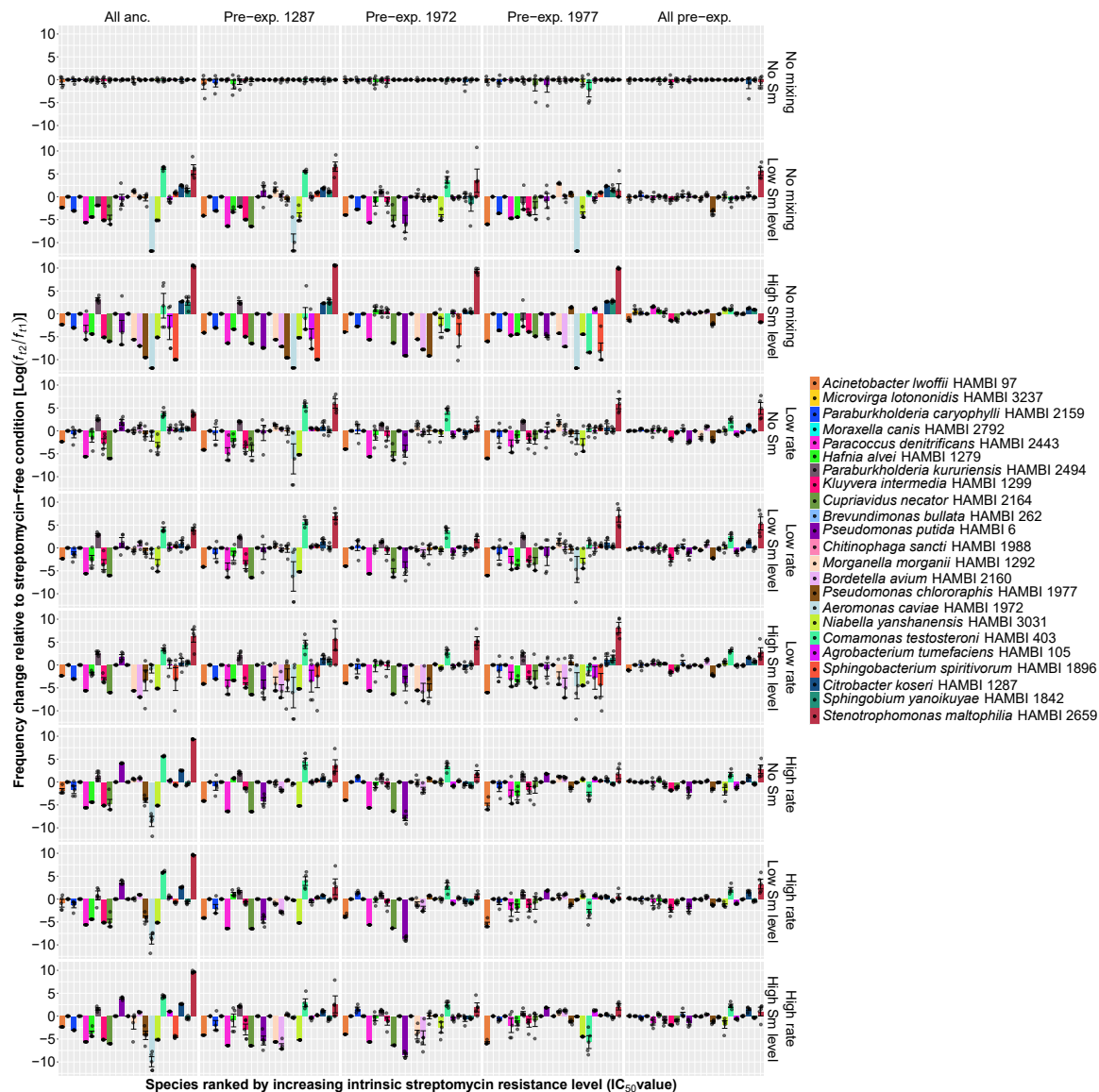
and *Pseudomonas chlororaphis* HAMB1 1977); and (5) pre-exposed populations used for all species. Within each pre-exposure treatment, the three streptomycin (Sm) disturbance patches (no, low, or high level) mixed at low or high rate (rows) have a shared history and can be identified by the replicate number shown on the x-axis. For instance, replicates D for each streptomycin level at low mixing rate in the first evolutionary treatment ('All ancestral'; three middle rows on the left) represent three patches that were mixed regularly and therefore resemble each other more than the other replicates in the same antibiotic level.





**Extended Data Fig. 2 | A t-SNE map showing *de novo* community clustering at the end-point of serial propagation experiment.** The experiment consisted of three patches exposed to no or two increasing levels of the model disturbance streptomycin ('Sm'; colors), exposed to no or two increasing levels of community mixing (rows), as well as configured into five different pre-exposure treatments (columns), with four replicate communities (shapes) for each unique treatment combination ( $N = 3 \times 3 \times 5 \times 4 = 180$  populations). The pre-exposure treatments consisted of no pre-exposure for any of the 23 species in the community

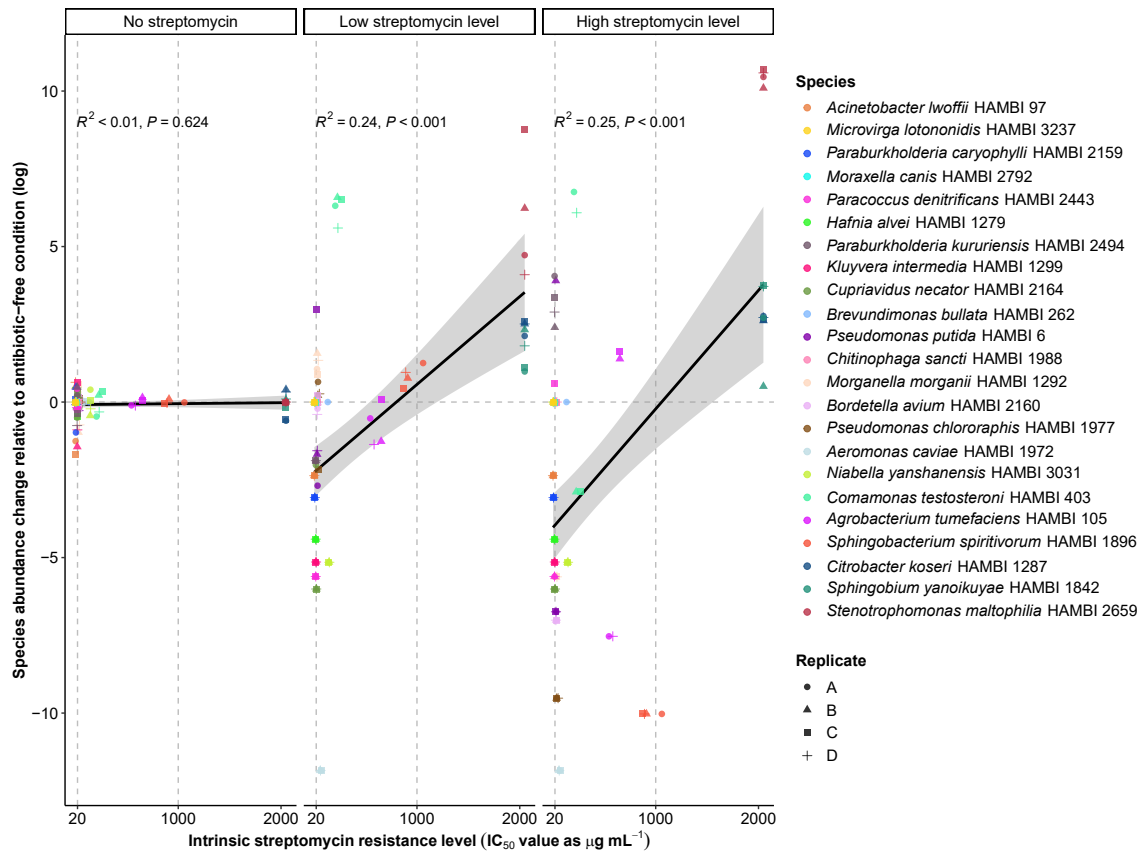
('All anc.'), a pre-exposed ('Pre-exp.') population for one of three abundant species (*Citrobacter koseri* HAMBI 1287, *Aeromonas caviae* HAMBI 1972, and *Pseudomonas chlororaphis* HAMBI 1977), and a community with pre-exposed populations of all community members. All data points originate from the same t-SNE analysis and have been separated into panels (with same arbitrary axis units) only for the sake of visual clarity of the effects of experimental treatments on compositional divergence between communities.



**Extended Data Fig. 3 | Effect of disturbance, community mixing and pre-exposure on community composition.** Frequency of each species relative to the frequency of the same species in the pre-exposure treatment specific control condition with no streptomycin ('Sm') or community mixing (that is, top panel) at the end-point of 46-day serial passage experiment (mean with s.e.m. for 4 replicates for each unique treatment combination). The data points in the control condition (top row) represent variation of the four control replicates around their mean (zero) and therefore deviate from zero. Columns show data

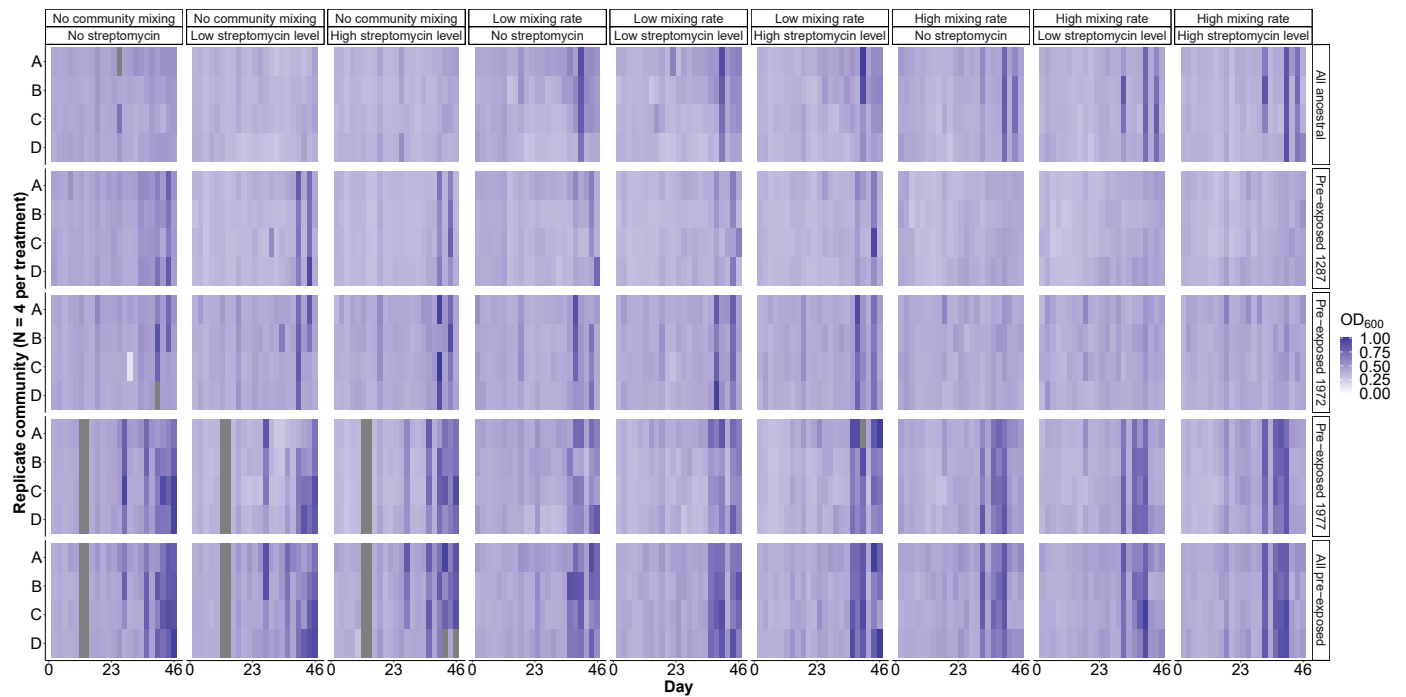
for the five pre-exposure treatments from left to right as follows: (1) ancestral populations used for all species ('All anc.');

(2–4) a population used for one of three abundant species that had been pre-exposed ('Pre-exp.'): to the disturbance (HAMBI Culture Collection code indicated in column label: *Citrobacter koseri* HAMBI 1287, *Aeromonas caviae* HAMBI 1972, and *Pseudomonas chlororaphis* HAMBI 1977); and (5) pre-exposed populations used for all species. Rows show data for the three streptomycin disturbance conditions (no, low, and high level) nested within each of three community mixing rates (no, low, or high level).



**Extended Data Fig. 4 | Relationship between intrinsic streptomycin level and frequency change of 23 species in model community at different streptomycin levels in the absence of community mixing or streptomycin pre-exposure (N = 23 species in 4 replicate communities for each streptomycin level).**

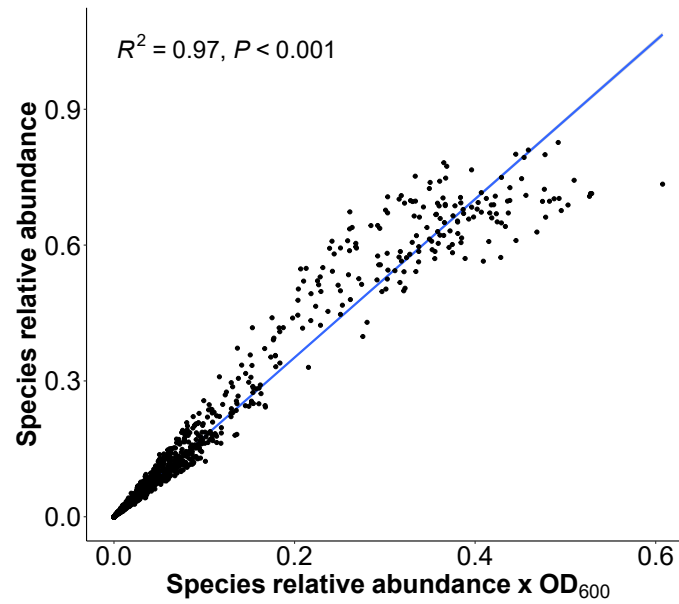
The coefficient of determination ( $R^2$ ) and  $P$ -value of linear regression fits to data for both streptomycin levels are indicated within the subplots. Data are presented as mean values  $\pm$  SEM.



**Extended Data Fig. 5 | Community biomass (optical density, OD, at 600 nm wavelength) for each individual population ( $N=180$ ) over time during 46-day serial propagation community experiment.** Grey bars indicate missing data owing to technical failure. The columns show the three community mixing and streptomycin (model disturbance) treatments, and the rows show the five

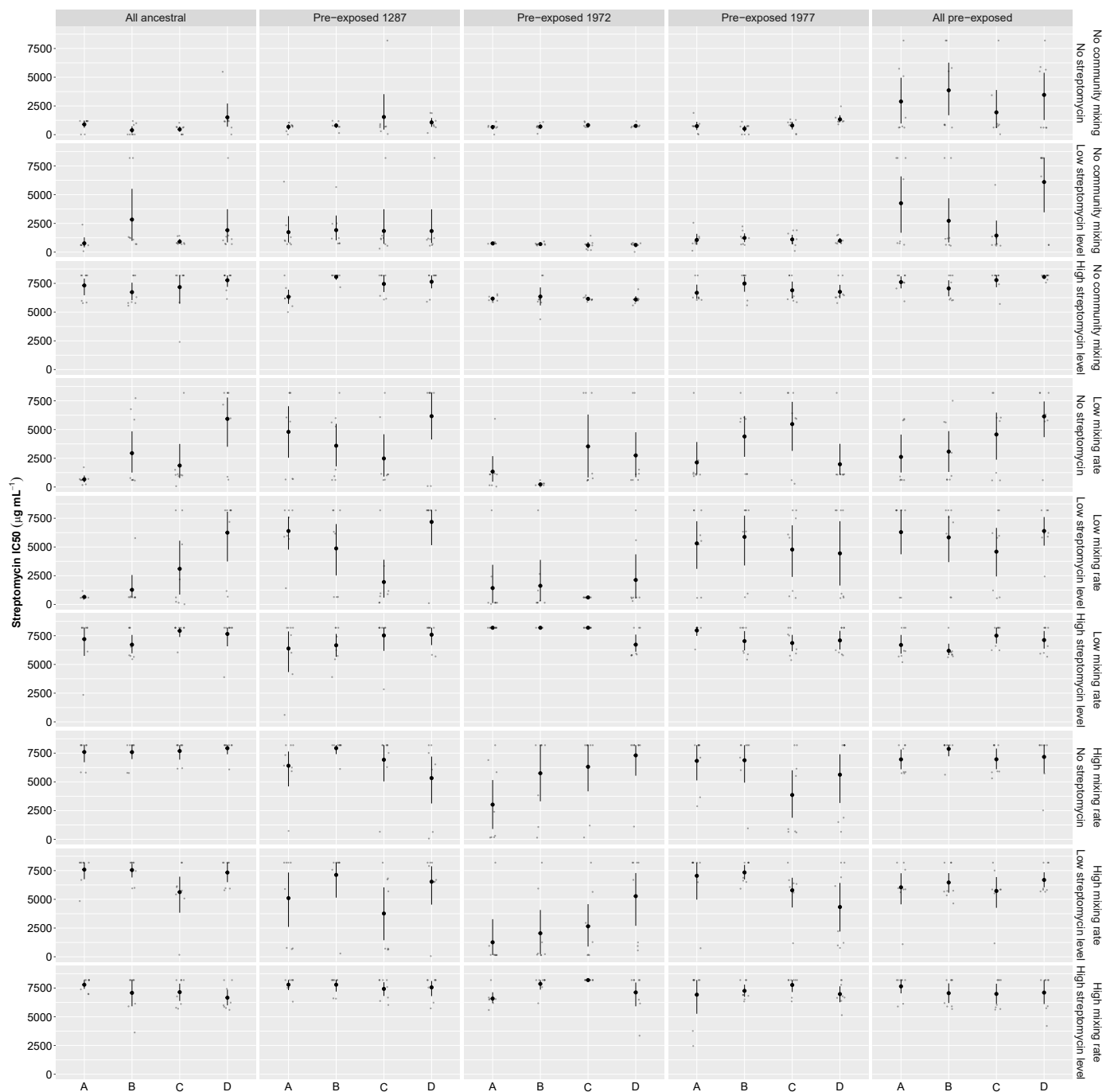
pre-exposure treatments. The codes in the pre-exposed treatments refer to the University of Helsinki HAMB1 culture collection codes of the following species: *Citrobacter koseri* HAMB1 1287, *Aeromonas caviae* HAMB1 1972, and *Pseudomonas chlororaphis* HAMB1 1977. The  $x$ -axis indicates time in days, and the  $y$ -axis indicates the experimental replicate in question.





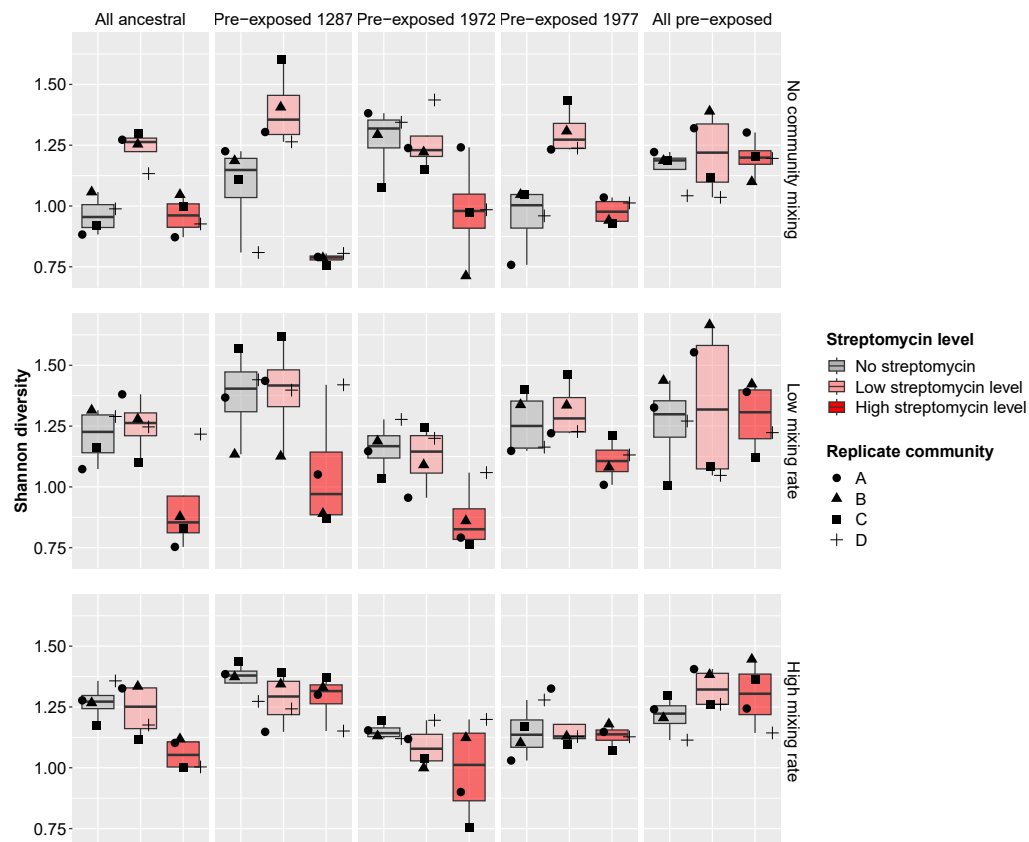
**Extended Data Fig. 6 | Relationship between relative and absolute species abundance.** The y-axis shows the relative abundance of each of the 23 model community species at the experimental end-point ( $N = 180$  communities  $\times$  23 species). The x-axis shows the absolute abundance of the species, such that the relative abundance has been multiplied by the community biomass quantified as

the mean optical density (OD) value at 600 nm wavelength of the five final time points in the experiment (see Extended Data Fig. 5 above). The coefficient of determination ( $R^2$ ) and  $P$ -value of a linear regression fit to the data are indicated within the figure.



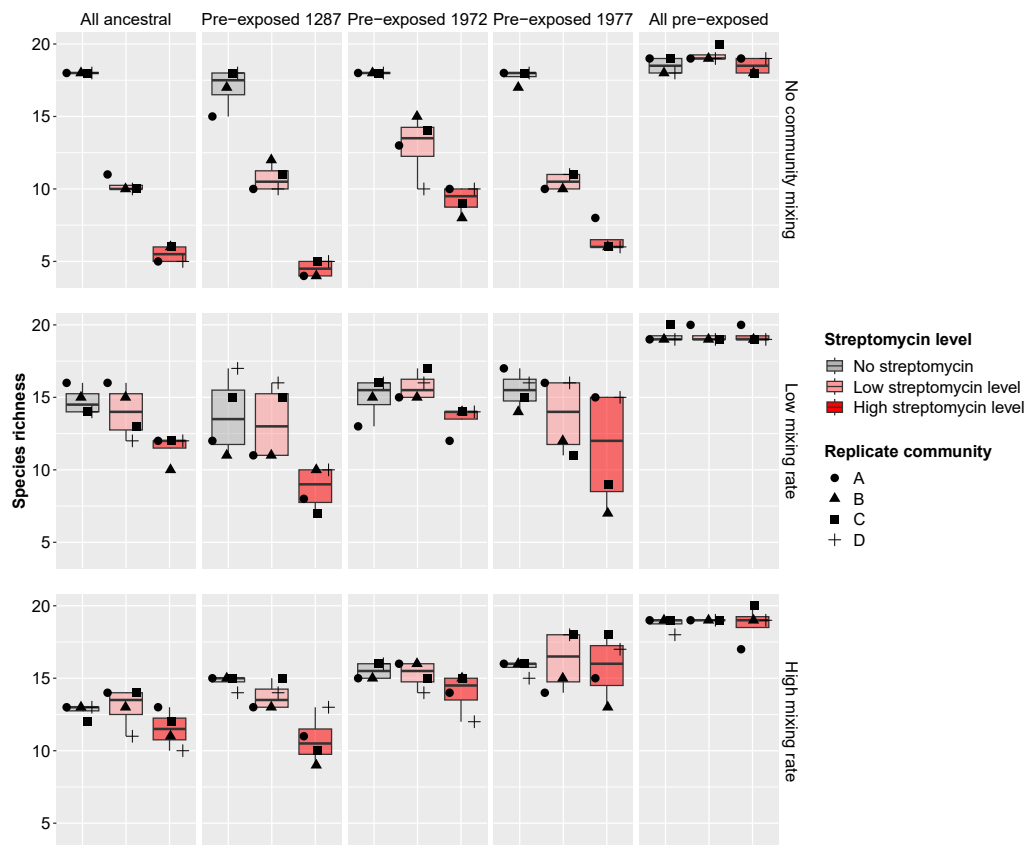
**Extended Data Fig. 7 | Effect of disturbance, community mixing and pre-exposure on disturbance resistance.** Half maximal inhibitory concentrations ( $IC_{50}$ ) for the model disturbance streptomycin are indicated for eight clones isolated from each population at the experimental end-point (mean with bootstrapped 95% confidence intervals). The data is considered to represent the  $IC_{50}$  values of dominant community members as the species identity of the clones was not determined. The pre-exposure treatments (columns) consisted

of no pre-exposure for any of the 23 species in the community ('All ancestral'), a pre-exposed population for one of three abundant species (*Citrobacter koseri* HAMB1 1287, *Aeromonas caviae* HAMB1 1972, and *Pseudomonas chlororaphis* HAMB1 1977), and a community with pre-exposed populations of all community members. Within each pre-exposure treatment, the three antibiotic disturbance patches mixed at low or high rate (rows) have a shared history and can be identified by the replicate letter code in the x-axis.



**Extended Data Fig. 8 | Shannon diversity of communities at end-point of serial propagation experiment ( $N=180$ ).** The data is depicted as Shannon diversity for three patches with different disturbance regimes (no, low or high streptomycin level) at no, low or high rate of community mixing (rows) between the three patches ( $N=4$  replicates per unique treatment combination). Columns show data for the five pre-exposure treatments as follows: (1) ancestral strains used for all species; (2–4) a population used for one of three abundant species that had been pre-exposed to the disturbance (HAMBI Culture Collection code indicated in column label: *Citrobacter koseri* HAMBI 1287, *Aeromonas caviae* HAMBI 1972, and

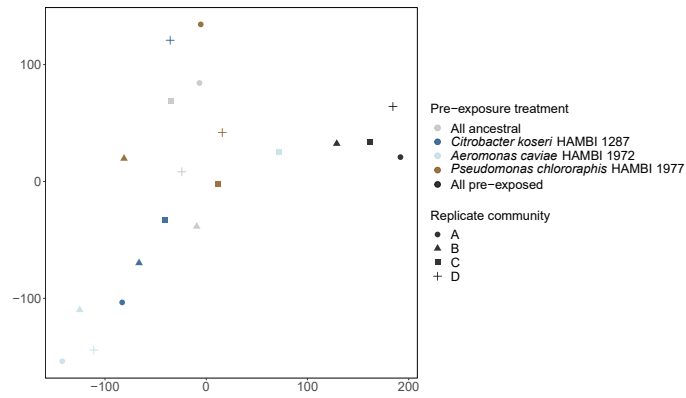
*Pseudomonas chlororaphis* HAMBI 1977); and (5) pre-exposed populations used for all species in the community. A model bacterial community consisting of 23 gram-negative species was employed. Box plot bars and shapes indicate medians and data points, respectively. The boxes indicate the interquartile range (25–75th percentile) and whiskers indicate lower and upper quartiles minus or plus 1.5 times the interquartile range. Within each pre-exposure treatment, the three antibiotic perturbation patches mixed at low or high rate have a shared history and can be identified by the replicate number indicated by shape.



**Extended Data Fig. 9 | Species richness of communities at end-point of serial propagation experiment ( $N=180$ ).** The data is depicted as species richness for three patches with different disturbance regimes (no, low or high streptomycin level) at no, low or high rate of community mixing (rows) between the three patches ( $N=4$  replicates per unique treatment combination). Columns show data for the five pre-exposure treatments as follows: (1) ancestral strains used for all species; (2–4) a population used for one of three abundant species that had been pre-exposed to the disturbance (HAMBI Culture Collection code indicated in column label: *Citrobacter koseri* HAMBI 1287, *Aeromonas caviae* HAMBI 1972, and

*Pseudomonas chlororaphis* HAMBI 1977); and (5) pre-exposed populations used for all species in the community. A model bacterial community consisting of 23 gram-negative species was employed. Box plot bars and shapes indicate medians and data points, respectively. The boxes indicate the interquartile range (25–75th percentile) and whiskers indicate lower and upper quartiles minus or plus 1.5 times the interquartile range. Within each pre-exposure treatment, the three antibiotic perturbation patches mixed at low or high rate have a shared history and can be identified by the replicate number indicated by shape.





**Extended Data Fig. 10 | A t-SNE map showing *de novo* community clustering at the end-point of serial propagation experiment among the different pre-exposure treatments in the absence of streptomycin or community mixing ( $N = 5$  pre-exposure treatments  $\times$  4 replicate communities = 20 communities).**

The pre-exposure treatments consisted of no pre-exposure for any of the 23 species in the community ('All ancestral'), a pre-exposed population for one three abundant species, and a community with pre-exposed populations of all community members. The t-SNE axis units are arbitrary.

## Reporting Summary

Nature Portfolio wishes to improve the reproducibility of the work that we publish. This form provides structure for consistency and transparency in reporting. For further information on Nature Portfolio policies, see our [Editorial Policies](#) and the [Editorial Policy Checklist](#).

### Statistics

For all statistical analyses, confirm that the following items are present in the figure legend, table legend, main text, or Methods section.

- | n/a                                 | Confirmed  |
|-------------------------------------|--|
| <input type="checkbox"/>            | <input checked="" type="checkbox"/> The exact sample size ( $n$ ) for each experimental group/condition, given as a discrete number and unit of measurement  |
| <input type="checkbox"/>            | <input checked="" type="checkbox"/> A statement on whether measurements were taken from distinct samples or whether the same sample was measured repeatedly  |
| <input type="checkbox"/>            | <input checked="" type="checkbox"/> The statistical test(s) used AND whether they are one- or two-sided<br><i>Only common tests should be described solely by name; describe more complex techniques in the Methods section.</i>   |
| <input type="checkbox"/>            | <input checked="" type="checkbox"/> A description of all covariates tested   |
| <input checked="" type="checkbox"/> | <input type="checkbox"/> A description of any assumptions or corrections, such as tests of normality and adjustment for multiple comparisons   |
| <input type="checkbox"/>            | <input checked="" type="checkbox"/> A full description of the statistical parameters including central tendency (e.g. means) or other basic estimates (e.g. regression coefficient) AND variation (e.g. standard deviation) or associated estimates of uncertainty (e.g. confidence intervals) |
| <input type="checkbox"/>            | <input checked="" type="checkbox"/> For null hypothesis testing, the test statistic (e.g. $F$ , $t$ , $r$ ) with confidence intervals, effect sizes, degrees of freedom and $P$ value noted<br><i>Give <math>P</math> values as exact values whenever suitable.</i>                            |
| <input checked="" type="checkbox"/> | <input type="checkbox"/> For Bayesian analysis, information on the choice of priors and Markov chain Monte Carlo settings  |
| <input checked="" type="checkbox"/> | <input type="checkbox"/> For hierarchical and complex designs, identification of the appropriate level for tests and full reporting of outcomes  |
| <input checked="" type="checkbox"/> | <input type="checkbox"/> Estimates of effect sizes (e.g. Cohen's $d$ , Pearson's $r$ ), indicating how they were calculated  |

*Our web collection on [statistics for biologists](#) contains articles on many of the points above.*

### Software and code

Policy information about [availability of computer code](#)

Data collection

Data analysis

For manuscripts utilizing custom algorithms or software that are central to the research but not yet described in published literature, software must be made available to editors and reviewers. We strongly encourage code deposition in a community repository (e.g. GitHub). See the Nature Portfolio [guidelines for submitting code & software](#) for further information.

### Data

Policy information about [availability of data](#)

All manuscripts must include a [data availability statement](#). This statement should provide the following information, where applicable:

- Accession codes, unique identifiers, or web links for publicly available datasets
- A description of any restrictions on data availability
- For clinical datasets or third party data, please ensure that the statement adheres to our [policy](#)

Raw sequence data (fastq files) has been deposited in the NCBI Sequence Read Archive (SRA) under the accession PRJNA1126612 . All code and pre-processed data needed to reproduce the downstream analyses and figures are available in Zenodo: <https://doi.org/10.5281/zenodo.14015860>.

## Research involving human participants, their data, or biological material

Policy information about studies with [human participants or human data](#). See also policy information about [sex, gender \(identity/presentation\), and sexual orientation](#) and [race, ethnicity and racism](#).

|  |    |
|--|----|
| Reporting on sex and gender  | NA |
| Reporting on race, ethnicity, or other socially relevant groupings | NA |
| Population characteristics   | NA |
| Recruitment  | NA |
| Ethics oversight   | NA |

Note that full information on the approval of the study protocol must also be provided in the manuscript.

## Field-specific reporting

Please select the one below that is the best fit for your research. If you are not sure, read the appropriate sections before making your selection.

Life sciences  Behavioural & social sciences  Ecological, evolutionary & environmental sciences

For a reference copy of the document with all sections, see [nature.com/documents/nr-reporting-summary-flat.pdf](https://www.nature.com/documents/nr-reporting-summary-flat.pdf)

## Ecological, evolutionary & environmental sciences study design

All studies must disclose on these points even when the disclosure is negative.

|                          |  |
|--------------------------|--|
| Study description        | The main experiment in the study was a full-factorial serial passage experiment. The setup included five pre-exposure treatments (no species pre-exposed, one of three abundant species pre-exposed, or all species pre-exposed to increasing concentrations of antibiotic), three antibiotic patches (no antibiotic, low concentration, high concentration), three rates of community mixing between the three antibiotic patches (no mixing, mixing every three transfers, or mixing every six transfers), and four replicates per each unique treatment combination. The experiment for these communities ( $N = 5 \times 3 \times 3 \times 4 = 180$ ) was conducted for 46 days with serial transfer of 1% v/v every 48 h.   |
| Research sample          | Community size was measured over time for each of the 180 communities. 16S rRNA amplicon shotgun sequencing was performed to detect community composition at the experimental end-point ( $N = 180$ ). Each pre-exposed species was whole-genome sequenced and phenotyped to identify mutations and associated trait change. Experimental end-point communities were also studied for phenotypic change: For the strains used to initiate the main experiments, four replicate dose-response experiments were performed for each ancestral species (four clones per species) and 16 for each population of the three abundant pre-exposed species. For experimental end-point communities, and eight clones we isolated and phenotyped from each of the 180 communities (1,440 clones in total). |
| Sampling strategy        | The study focused on community change at the experimental end-point where all samples were measured. All samples were also measured regarding the genomic effects of antibiotic pre-exposure, but phenotyping focused on the three abundant species used in the pre-exposure treatments of the main experiment.  |
| Data collection          | The phenotypic data was collected and DNA extracted by Elizaveta Zakharova, who measured optical density over time and IC50 values for streptomycin for evolved strains and clones from experimental communities. The data was recorded in tab-delimited data files. Sequencing was carried out by a third party (Finnish Institute of Molecular Medicine, FIMM), and data was supplied to researchers in FASTQ file format.   |
| Timing and spatial scale | The data was collected in 2021-2022. The data pertains to communities and clones suspended in frozen animation that were either used to initiate the experiment, pre-exposed to the antibiotic prior to the experiment, or derive from the main 46-day serial passage experiment.  |
| Data exclusions          | Originally, the pre-exposure treatment included also the species <i>Pseudomonas putida</i> HAMBI 6, <i>Agrobacterium tumefaciens</i> HAMBI 105, and <i>Sphingobacterium spiritivorum</i> HAMBI 1896. However, whole-genome sequence analysis of the pre-exposed populations of these species used to initiate the serial passage experiment showed them to be contaminated with other pre-exposed species. They were therefore omitted from the analysis. This resulted in the levels of the pre-exposure treatment decreasing from 8 to 5, and the total number of experimental end-point communities analysed decreasing from 288 to 180.  |
| Reproducibility          | A full-factorial experimental design with 4 replicates for each unique treatment combination were used to inspect reproducibility of eco-evolutionary outcomes. All measurements were successful with no need to repeat experiments.   |
| Randomization            | A controlled full-factorial in vitro serial passage experiment was performed, starting each community with the same initial  |

- Randomization
- Blinding
- Did the study involve field work?  Yes  No

## Reporting for specific materials, systems and methods

We require information from authors about some types of materials, experimental systems and methods used in many studies. Here, indicate whether each material, system or method listed is relevant to your study. If you are not sure if a list item applies to your research, read the appropriate section before selecting a response.

### Materials & experimental systems

- n/a  Involved in the study
- Antibodies
- Eukaryotic cell lines
- Palaeontology and archaeology
- Animals and other organisms
- Clinical data
- Dual use research of concern
- Plants

### Methods

- n/a  Involved in the study
- ChIP-seq
- Flow cytometry
- MRI-based neuroimaging

## Animals and other research organisms

Policy information about [studies involving animals](#); [ARRIVE guidelines](#) recommended for reporting animal research, and [Sex and Gender in Research](#)

- Laboratory animals
- Wild animals
- Reporting on sex
- Field-collected samples
- Ethics oversight

Note that full information on the approval of the study protocol must also be provided in the manuscript.

## Plants

- Seed stocks
- Novel plant genotypes
- Authentication